How to date a crocodile: estimation of neosuchian clade ages and a comparison of four time-scaling methods

by SEBASTIAN S. GROH[1,2] (iD), PAUL UPCHURCH[1] (iD), PAUL M. BARRETT[2,3] (iD) *and* JULIA J. DAY[4] (iD)

[1]Department of Earth Sciences, University College London, Gower Street, London, WC1E 6BT, UK; sebastian.groh@ucl.ac.uk
[2]Department of Earth Sciences, Natural History Museum, Cromwell Road, London, SW7 5BD, UK
[3]Department of Cell & Developmental Biology, University College London, Gower Street, WC1E 6BT, London, UK
[4]Department of Genetics, Environment & Evolution, University College London, Gower Street, London, WC1E 6BT, UK

Abstract: Clade ages within the crocodylomorph clade Neosuchia have long been debated. Molecular and morphological studies have yielded remarkably divergent results. Despite recent advances, there has been no comprehensive relative comparison of the major time calibration methods available to estimate clade ages based on morphological data. We used four methods (cal3, extended Hedman, smoothed ghost lineage analysis (sGLA) and the fossilized birth–death model (FBD)) to date clade ages derived from a published crocodylomorph supertree and a new neosuchian phylogeny. All time-scaling methods applied here agree on the origination of Neosuchia during the Late Triassic or Early Jurassic, and the presence of the major extant eusuchian groups (Crocodyloidea, Gavialoidea, Alligatoroidea and Caimaininae) by the end of the Late Cretaceous. The number of distinct lineages present before the K/Pg boundary is less certain, with support for two competing scenarios in which Crocodylinae, Tomistominae and Diplocynodontinae either: (1) diverged from other eusuchian lineages before the K/Pg boundary; or (2) evolved during a 'burst' of diversification after the K/Pg event. Cal3 and FBD proved to be the most suitable methods for time-scaling phylogenetic trees dominated by fossil taxa. Extended Hedman estimates are substantially older than the others, with larger standard deviations and a strong sensitivity to taxon sampling and topological changes; sGLA has similar problems. We conclude that a detailed understanding of phylogenetic relationships, tree reconstruction methods, and good taxonomic coverage (in particular the inclusion of the oldest taxon in each clade) is essential when evaluating the results of such dating analyses.

Key words: divergence estimation, cal3, Crocodylia, extended Hedman, Neosuchia.

ORIGINATION time estimation is essential when determining the tempo of clade evolution, and serves as the basis for a range of downstream studies, such as correlating clade origination with climatic or palaeogeographical changes (e.g. Springer *et al.* 2011; Hastings *et al.* 2013; Patiño & Vanderpoorten 2015). Significant problems with clade age estimation can occur when the datasets in question are based largely, or solely, on either fossil or extant taxa. When fossil taxa dominate a dataset, the incorporation of no (or limited) molecular sequences can ignite major debates over tree dating and clade origination times (e.g. for placental mammals: O'Leary *et al.* 2013; dos Reis *et al.* 2014). Such morphology-dominated datasets are often difficult or impossible to analyse using node-based molecular clock methods, leaving palaeobiologists largely dependent on a literal reading of the fossil record (Turner *et al.* 2017). Over the past three decades, however, a number of methods suitable for estimating clade ages in morphology-based phylogenies have been developed. In some cases, these were originally created for use with molecular phylogenies, but subsequently adapted for morphological datasets. These include methods using Bayesian inference, such as the fossilized birth–death model (FBD) (Stadler 2010; Heath *et al.* 2014). The FBD is one of the models that allows for the incorporation of fossils as tips in phylogenetic trees and randomises both speciation and extinction probabilities over time. It was further refined to allow more flexibility for fossil assignments and model parameters by Gavryushkina *et al.* (2014). Although using these serially sampled birth–death models can lead to long ghost lineages (Turner *et al.* 2017), incorporating birth, death and sampling rates renders more accurate results than those yielded by models without these rates, because the latter tend to produce estimates that are too old (Matzke & Wright 2016).

In addition to Bayesian approaches, other methods for origination time estimation have been proposed specifically for use with phylogenies with high proportions of

fossil taxa. In contrast to node-dating approaches, several *a posteriori* dating methods use the ages assigned to tips on a pre-defined phylogeny. The first methods to apply this approach were developed in the 1990s, as extensions and formalizations of the traditional palaeobiological minimum age estimation approach. Crucially, however, these took phylogenetic topology into account and created the concept of 'ghost ranges' for implied but missing portions of the fossil record (Norell *et al.* 1992; Smith 1994). These basic algorithms used the ages of taxa bracketing a node to assign a minimum age to that node. However, this can lead to the inference of long ghost ranges (Turner *et al.* 2017) and branches of zero length (Hunt & Carrano 2010). Several methods for scaling these branches have now been developed (e.g. Ruta *et al.* 2006; Brusatte *et al.* 2008; Laurin *et al.* 2009; Brusatte 2011) and these algorithms are still in use in several stratigraphic time-scaling approaches (e.g. Bell & Lloyd 2014). Following the terminology of Turner *et al.* (2017), this set of methods will be referred to as 'ghost lineage analysis' (GLA) henceforth, and the 'equal' option (for distributing a cluster of zero-length branches, see below) as 'smoothed ghost lineage analysis' (sGLA; Turner *et al.* (2017)). These algorithms can be problematic because they do not fully take into account the stochastic uncertainty of node ages that is contained within the stratigraphic record, instead incorporating only a portion of uncertainty related to occurrence time. Newer methods for stochastic age estimation have been introduced, including cal3 (Bapst 2013) and, most recently, 'extended Hedman' (EH) (Lloyd *et al.* 2016), based on the extension and modification of a Bayesian method to date single nodes proposed by Hedman (2010).

A comparison of these four methods (FBD, sGLA, Cal3 and EH) has been strongly encouraged by previous authors (Bapst *et al.* 2016). However, although earlier works have applied two or more of these methods (Bapst & Hopkins 2017; Puttick *et al.* 2017; Soul & Friedman 2017; Benson *et al.* 2018; Allen *et al.* 2019; Godoy *et al.* 2019), to date there has been no simultaneous or in-depth comparison of all four.

Neosuchia is a key vertebrate group with a high proportion of extinct species (Sereno *et al.* 2001; Andrade *et al.* 2011). This is a crocodylomorph clade that encompasses all extant species (alligators, caimans, crocodiles, gharials: <30 spp). and numerous extinct taxa (>300 spp) (Brochu 2003; Grigg *et al.* 2015; Mannion et al. 2019). In addition, Neosuchia contains a large number of extinct crocodylian crown-group taxa (74% of the neosuchian species in our dataset), a data source usually excluded in molecular analyses. Since the earliest clade age estimations for Neosuchia (Brochu 2000), numerous molecular and morphological studies using different dating algorithms (including node age estimations) have been published (Table 1). For most groups, there is a stark difference in

the node age estimates obtained from molecular and morphological methods, with molecular estimates tending to be younger (Brochu 2000), as exemplified by the dates for Crocodylinae (Table 1). These younger molecular estimates can be explained by all terminal taxa being extant, an insufficient number of calibration points (e.g. only one calibration point within Neosuchia: Roos *et al.* 2007) and rather young age restrictions for older clades (e.g. 90 and 100 million years ago (Ma) for the origination of Crocodylia: Oaks 2011). Furthermore, the different placements of *Gavialis* and *Tomistoma* within competing phylogenies, and the absence of entirely extinct clades (e.g. Diplocynodontinae) and older extinct species of extant lineages (e.g. non-extant crocodyline species) from molecular studies, tend to bias clade age estimates towards younger dates.

One previous study used a GLA method, cal3 and EH to date crocodylomorph trees in order to evaluate the fit of different models of body size evolution, but because of their similarity to FBD results, these additional date estimates were not discussed further (Godoy *et al.* 2019). So far, no study has attempted to date the origination times of all major neosuchian clades comprehensively using different methods.

The main goals of this study are: (1) to obtain age estimates of origination times of key clades in neosuchian evolution, which can further enable the identification and testing of macroevolutionary patterns, such as assessing the clade's response to the K/Pg mass extinction; (2) to apply the four different time-scaling methods to the same set of topologies in order to compare the results of newer, stochastic time-scaling methods (cal3, EH) with more established ones; and (3) to assess the relative differences between these four methods (e.g. non-random patterns in the distributions of node age estimations) and their sensitivity to taxon sampling and topological variance. To do this, we present a new neosuchian phylogeny that updates and expands upon previous work (Groh *et al.* 2020). We then apply the four major *a posteriori* methods (cal3, EH, sGLA (one of the GLA methods) and FBD) to the resulting evolutionary trees. For the purpose of comparing our results with the age estimates based on previously published neosuchian phylogenies, we also apply the same four time-scaling methods to the crocodylomorph supertree presented by Stockdale & Benton (2021). The node age estimates are then compared statistically, and we discuss them in the context of previous work on neosuchian evolution.

MATERIAL AND METHOD

Phylogenetic trees

The new phylogenetic topologies used in this study were derived from analysis of a modified version of the dataset

TABLE 1. Previous neosuchian origination time estimates.

	Andrade et al. (2011)	Martin et al. (2010)	Oaks (2011)*	Puértolas et al. (2011)	Roos et al. (2007)*	Salisbury et al. (2006)	Turner et al. (2017)	Lee & Yates (2018)	Godoy et al. (2019)
Program/Method	?‡	?‡	BEAST	PAST	Tree-Finder	GLA	GLA, sGLA, FBD	FBD†	FBD
Neosuchia	208	–	–	–	–	–	209–189	–	200–195
Eusuchia	150	130	–	130	–	120	172.8–145.1	138	145–135
Tethysuchia	148	146	–	–	–	–	187–156	–	190–174
Goniopholididae	197	–	–	–	–	–	197–184	–	190
Crocodylia	73	81	100.0–81.08	90	103–97	89	101.7–77.1	100	125–115
Gavialoidea	–	71	–	79	–	78	89–68	–	90
Brevirostres	–	80	–	86	–	87	99–75	–	–
Crocodyloidea	–	80	–	73	–	73	–	81	82
Crocodylidae	–	80	69.91–39.85	61	49–47	59	–	37	70
Crocodylinae	–	–	39.85–19.31	43	29–28	45	–	22	–
Tomistominae	–	–	–	57	–	57	–	–	60
Alligatoroidea	–	80	–	85	–	82	–	93	90
Diplocynodontinae	–	–	–	–	–	50	–	48	–
Globidonta	–	–	69.53–61.76	84	71–66	80	–	83	85
Alligatorinae	–	–	58.28–35.29	70	53–47	70	–	70	80
Caimaninae	–	–	39.84–20.14	57	41–31	57	–	55	58

Ages given in millions of years. If not mentioned explicitly in the text or supplementary information, the values were taken from the summary figures.

*Molecular studies

†Total evidence Bayesian tip dating, although 95% was not given

‡Actual statistical method used for calibration unclear; figure descriptions state that they were 'stratigraphically calibrated'

presented by Groh *et al.* (2020). Complete information on the original phylogeny, including details of character revision and construction according to the schemes laid out in Sereno (2007) and Brazeau (2011) (but see Sookias (2020) for an argument against splitting composite multistate characters) can be found in the aforementioned publication and are not repeated herein. Modifications to the Groh *et al.* (2020) dataset included the incorporation of 12 additional taxa based on their published descriptions, which were selected to improve the sampling of previously under-sampled groups and to ensure that the oldest-known taxon from each of the major clades was represented (Table 2). Furthermore, we revised the character state scores for 11 species based on additional fossil material (Groh *et al.* 2022, phylogenetics): *Bernissartia fagesii* (Buscalioni & Sanz 1988); *Borealosuchus formidabilis* (Brochu 1997); *Brachychampsa montana* (Norell *et al.* 1994); *Comahuesuchus brachybuccalis* (Martinelli 2003); *Dyrosaurus phosphaticus* (Jouve *et al.* 2005); *Eutretauranosuchus delfsi* (Smith *et al.* 2010); *Leidyosuchus canadensis* (Wu *et al.* 2001a); *Maroccosuchus zennaroi* (Jouve *et al.* 2015); *Notosuchus terrestris* (Pol 2005; Fiorelli & Calvo 2008); *Sarcosuchus imperator* (Sereno *et al.* 2001); and *Shamosuchus djadochtaensis* (Pol *et al.* 2009).

We deleted six characters and added two new ones (see Groh *et al.* 2022 (phylogenetics) for detailed changes to the character list). The final dataset comprised 565 characters (82 continuous and 483 discrete) for 122 taxa (full character list in Groh *et al.* 2022, phylogenetics). We used parsimony analyses, following the protocol laid out in Groh *et al.* (2020) (full TNT protocol in Groh *et al.* 2022, phylogenetics). In brief, two versions of the dataset were analysed: the full version with continuous and discrete characters; and a discrete version where all continuous characters were rediscretized (i.e. scored in discrete character states of '0' or '1' instead of ratios based on measurements). Character weights were multiplied by 1000 to adjust for the different weighting of continuous characters (see Groh *et al.* (2020) for details). All phylogenetic analyses were carried out in TNT v.1.5 (Goloboff & Catalano 2016), using New Technology Search with extended implied weighting under $k = 3$ (Goloboff 2014) followed by a traditional search. The analyses were not constrained for the known molecular topologies, because doing so clustered all the long-snouted taxa together in a stratigraphically unlikely clade. Additionally, we did not make use of Bayesian phylogenetic methods, because previous Bayesian analyses of the same dataset yielded trees

TABLE 2. Taxa added to our dataset and their taxonomic affinities, based on their descriptions in the literature.

Taxon name	References	Taxonomy
Aegisuchus witmeri	Holliday & Gardner (2012)	Aegyptosuchidae
Aegyptosuchus peyeri	Stromer (1933)	Aegyptosuchidae
Aprosuchus ghirai	Venczel & Codrea (2019)	Atoposauridae
Calsoyasuchus valliceps	Tykoski *et al.* (2002)	Goniopholididae
Brachychampsa sealyi	Williamson (1996)	Alligatoroidea
Batrachomimus pastosbonensis	Montefeltro *et al.* (2013)	Paralligatoridae
Knoetschkesuchus guimarotae	Schwarz & Salisbury (2005)	Atoposauridae
Knoetschkesuchus langenbergensis	Schwarz *et al.* (2017)	Atoposauridae
Meridiosaurus vallisparadisi	Fortier *et al.* (2011)	Tethysuchia
Portugalosuchus azenhae	Mateus *et al.* (2018)	Eusuchia
Rugosuchus nonganensis	Wu *et al.* (2001*a*)	Paralligatoridae
Susisuchus jaguaribensis	Fortier & Schultz (2009)	Susisuchidae

with very low resolution that would be unsuitable for clade age estimation (Groh *et al.* 2020).

After the initial tree analyses, four taxa were identified in stratigraphically unlikely positions that differed in their phylogenetic affinities from previous studies. These are: *Sarcosuchus imperator* (a tethysuchian: Sereno *et al.* 2001; Hastings *et al.* 2010, 2014) and *Arambourgia gaudryi* (an alligatorid: Brochu 1999; Martin & Lauprasert 2010) that were found in positions as sister taxa to all other neosuchians because of an unusual combination of characters and poor preservation in parts of the examined material; *Rhamphosuchus crassidens* (a Miocene tomistomine: Piras 2007) placed as an early diverging gavialoid because of the fragmentary nature of the specimen; and *Susisuchus jaguaribensis* (a susisuchid or early neosuchian: Fortier & Schultz 2009; Turner & Pritchard 2015) placed as an early crocodyloid because of the low number of characters that could be scored (18% of all characters including no continuous ones) and the similarity of several skull table characters with those of early crocodyloids. To test for the influence of such taxa in 'rogue' placements, the subsequent dating analyses were carried out on two tree sets: the complete trees and those with the four rogue taxa in question removed from the topology.

To compare the results derived from our new phylogeny to those based on previously published neosuchian topologies, we also analysed the most recent crocodylomorph supertree, constructed by Stockdale & Benton (2021). This topology was pruned so that it contained

neosuchian taxa only, matching the same five outgroup taxa used in Groh *et al.* (2020). We used two versions of this trimmed tree in order to account for the different placement of Thalattosuchia in other neosuchian phylogenies (e.g. Wilberg 2015): one with Thalattosuchia included within Neosuchia, as the sister group to Tethysuchia; and one with Thalattosuchia placed outside Neosuchia. The resulting trees contained 171 and 148 neosuchian taxa, respectively.

Stem-based and node-based definitions and their influence on clade age estimation

One issue that has received little prior attention is the potential for creating artefactual discrepancies in proposed origination dates, because of the way in which phylogenetic clade names are defined. Phylogenetic definitions are often either stem-based or node-based, and our own definitions are a mix of both (Groh *et al.* 2022, phylogenetics). In this paper, we usually refer to 'origination times', 'node age estimates' or 'clade age estimates'. These describe the age estimates for the node that represents the most recent common ancestor (MRCA) of the currently-sampled species within a given clade X, irrespective of whether its definition is stem-based or node-based. Wherever we describe the timing of divergence of a clade X from its sister clade Y, we use the term 'divergence time' (Fig. 1)

Taxon ages

Terminal taxon ages were taken from the Paleobiology Database (PBDB) (https://paleobiodb.org; accessed 15 May 2020) and adjusted for the more recently revised ages established in the International Chronostratigraphic (ICS) chart (Cohen *et al.* 2013; v.2020/03). Several species
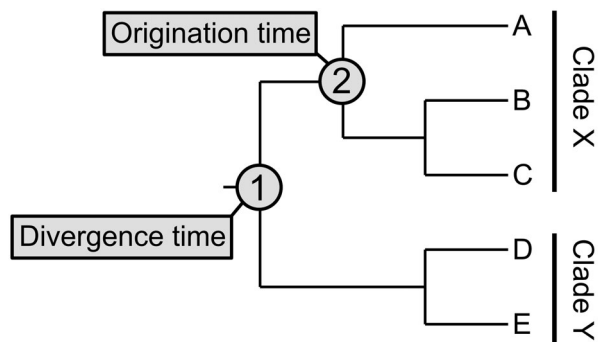

FIG. 1. Schematic explanation of the difference between the terms 'origination time' and 'divergence time' for hypothetical clades X and Y.

(such as *Alligator mcgrewi*) are from formations that were categorized using North American Land Mammal Ages in their original publications. For methods requiring non-overlapping time bins (e.g. cal3), occurrences were integrated into the existing ICS standard stages and epochs (the complete time bin list is available in Groh *et al.* 2022, timescaling). The Holocene was used as the time bin for extant taxa that currently lack a fossil record.

A singleton is defined herein as a taxon that includes one or multiple specimens from a single stratigraphic horizon. The presence of such singletons can falsely limit age estimates to smaller ranges and lead to inaccurate rate estimations in methods such as cal3 (Foote 1997; Bapst 2014). The modified Groh *et al.* and Stockdale & Benton (2021) datasets contain 31% and 41% singletons, respectively. Thus, the ages (e.g. expressed as presence during a given geological stage) for singleton taxa do not correspond to genuine stratigraphic ranges because they are point occurrences in time, so any inferred age range (based on the total age range of their parent rock unit) represents uncertainty in their fossil record. For the purpose of this study, non-singleton taxa were treated as though their stratigraphic ranges were fully known. The difference between singletons and non-singleton taxa was addressed in the following way in our analyses:

1. For the time bins used in cal3 and sGLA, singleton species were assigned time bins that covered their full potential stratigraphic range, because both methods choose the ages randomly from the assigned ranges. Non-singleton taxa were assigned the time bins that represented the uncertainty surrounding their first appearance (e.g. a species with occurrences in early and late Maastrichtian deposits would be assigned an early Maastrichtian time bin, because it cannot have originated later than the early Maastrichtian). For the rates calculation in cal3, non-singleton taxa were given full time bins covering their entire stratigraphic ranges.

2. For FBD, the midpoint age of a taxon's potential stratigraphic range was used, because use of uniform distributions for ages (such as in Lee & Yates 2018) led to younger species being dated tens of millions of years older than their actual occurrence ranges.

3. For EH, the median time bin of a taxon's potential stratigraphic range was used. In the case of a stratigraphic range spanning an even number of time bins, the later of the two median time bins was used.

A full list of taxon ages is available in Groh *et al.* (2022, timescaling).

Origination time estimation methods

To enable comparisons between the different approaches to tree dating, four different methods were applied to each of the phylogenetic trees produced by the protocols outlined above. All analysis scripts are available in Groh *et al.* (2022, timescaling).

Cal3

Cal3 is an *a posteriori* time-scaling method first described by Bapst (2013), and further elaborated in Bapst (2014). Instead of carrying out a single clade age estimation, cal3 employs repeated stochastic sampling of node ages from a given distribution. To create this distribution of possible node ages, three different rates were defined *a priori*: branching (= speciation) rate, extinction rate and sampling rate, using likelihood functions (Foote 1997). This prior rate estimation is problematic without using an already time-scaled phylogeny as a basis. In addition, it is influenced by the presence of singletons, because these can artificially increase the estimates of branching and extinction rates (which are usually assumed to be equal) (Bapst 2013, 2014). However, only 31% or 41% of the taxa in our datasets are singletons (see above) which compares favourably with those in which the percentage is higher (pterosaurs; 71.6%; Andres 2012) or unknown (dinosaurs; Lloyd *et al.* 2016); this problem should therefore be less severe when working with the neosuchian fossil record.

Cal3 and the algorithms used to estimate its rates are implemented in the R package `paleotree` (Bapst 2012) and were executed in R v.4.0.4 (R Core Team 2013). To estimate the branching, extinction and sampling rates, the function `make_durationFreqDisc` was applied; this constructs models of the observed taxon duration frequencies in given discrete time intervals using the likelihood functions for rate estimation by Foote (1997) as a basis. Following Bapst's recommendations written in the annotated cal3 code, artificial time intervals were generated, dividing each time period from the ICS chart into smaller, equal-length, time bins of 2–3 million years (myr). Rate estimation using these artificial time bins yielded the following rates (in species per million years) that were employed in the subsequent dating analyses: (1) branching rate = 0.1727298; (2) extinction rate = 0.1727298; and (3) sampling rate = 0.2618742. For clade age estimation, the original ICS time units were used.

Each topology was analysed 1000 times to obtain a distribution of different node age estimates. Node ages were extracted using the functions `mrca` and `branching.times` in the R package `ape` (Paradis & Schliep 2019).

Extended Hedman

Whole tree extension of the Hedman algorithm ('extended Hedman' or EH) is an *a posteriori* time-scaling

method proposed by Lloyd *et al.* (2016), based on a Bayesian method for the dating of single nodes first described by Hedman (2010). This approach has been modified and adapted for dating all nodes within a tree by Lloyd *et al.* (2016) and makes use of the ages of successive outgroups to estimate posterior distributions for node ages. As such, additional outgroup ages have to be added to enable the dating of all nodes in the target phylogenetic trees.

We implemented a modified version of the EH script supplied by Lloyd *et al.* (2016) in R v.4.0.4. (R Core Team 2013) to sample all node ages (instead of a selected few) and time-scale a tree topology with the mean ages (complete script in Groh *et al.* 2022, timescaling). Ten new outgroup ages were added to each tree (Table 3). Replacing these outgroup ages with older or younger ages did not lead to significant differences in the dates obtained (Groh *et al.* 2022, timescaling). The time bins in the occurrence file corresponded to official ICS time units (Cohen *et al.* 2013) and the actual number of occurrences for each species in every time bin (data from the PBDB) was used. Dates for each node were estimated 1000 times. Ages for specific nodes were extracted using `mrca` and `branching.times` as outlined above.

Smoothed ghost lineage analysis. 'Ghost-Lineage-Analysis' (GLA) describes the simplest type of *a posteriori* clade age estimation analysis. Initially, each node is assigned a minimum age equal to that of the oldest member within the clade (Norell *et al.* 1992). However, the presence of

TABLE 3. Ages of additional outgroup taxa for use with extended Hedman dating in this study, based on the phylogenetic relationships in Nesbitt (2011).

Age (myr)	Taxon	Clade
201.3	*Terrestrisuchus gracilis*	Early Crocodylomorpha
208.5	*Dromicosuchus grallator*	Early Crocodylomorpha
208.5	*Rauisuchus tiradentes*	Rauisuchidae
227	*Saurosuchus galilei*	Loricata
237	*Batrachotomus kupferzellensis*	Loricata
237	*Gracilisuchus stipanicicorum*	Early Pseudosuchia
242	*Ticinosuchus ferox*	Suchia
242	*Turfanosuchus dabanensis*	Gracilisuchidae
247	*Proterosuchus fergusi*	Archosauriformes
251	*Prolacerta broomi*	Archosauromorpha

Ages given in millions of years (myr), based on those from the PBDB (https://paleobiodb.org; accessed 15 May 2020) and adjusted to be consistent with the ICS chart (Cohen *et al.* 2013).

several closely related fossil taxa of approximately the same age, can lead to the introduction of zero length branches and multiple extremely short branches when time scaling is applied. Therefore, temporally 'smoothed' GLA (sGLA) makes use of a modified version of an algorithm originally described by Ruta *et al.* (2006) wherein these zero length branches are assigned lengths by distributing them evenly across the time between the nodes with which they are associated. This algorithm was implemented by Brusatte (2011) and Lloyd *et al.* (2012). Although sGLA is influenced by clustered occurrences over time (Turner *et al.* 2017) and potentially biased towards minimum age estimates (Lloyd *et al.* 2016), it has been applied widely because it is implemented in the R packages `paleotree` (Bapst 2012) and `strap` (Bell & Lloyd 2014). In our implementation of sGLA, the time bins used were the same as in the cal3 analysis. The 'equal' option of `bin_timePaleoPhy` was enabled in order to produce sGLA dated trees, rather than simple GLA ones. sGLA was run with three different vartime variables (= minimum time by which the root age is adjusted): vartime = 1, 5 and 10 for the first analysis. The results proved similar for all three, with notable differences in the obtained ages (all <5% of the total age) observed only in the five nodes closest to the root (see Groh *et al.* 2022, timescaling). Therefore, vartime = 1 was used for the analyses evaluated here. Each analysis was looped to carry out 1000 estimates for each most parsimonious tree (MPT). `ape` (Paradis & Schliep 2019) was used to extract node ages.

Fossilized birth–death model. The FBD model was developed by Stadler (2010) and Heath *et al.* (2014) and further expanded by Gavryushkina *et al.* (2014). It is part of BEAST2 (Bouckaert *et al.* 2014) and a number of other software packages that implement Bayesian methods. It allows for the direct incorporation of fossils into Bayesian age estimation models, randomizing both speciation and extinction probabilities over time. Depending on the tree, the performance of FBD is influenced little by additional node calibrations (Matzke & Wright 2016) but the estimation of the root age has been shown to increase in accuracy as more fossils are incorporated close to the root (Püschel *et al.* 2020). To keep the results of this method comparable to the three other time scaling methods used here, nodes were not additionally constrained, and no tree building was carried out in BEAST2, restricting the analysis to the previously supplied MPTs. Log normal priors were used throughout the analysis, with 200.3 as offset for the original tree (corresponding to the age of the oldest taxon) and M = 21.0, S = 1.0. Diversification rate was set to 1.0, turnover and sampling rates to 0.5, and Rho was 0.7. Each MPT obtained during the phylogenetic analysis was inserted separately into the xml file

generated by BEAUTi v.2.4.8 (part of the BEAST2 package). Because analysis of the rediscretized modified Groh *et al.* dataset yielded too many MPTs to be analysed individually by BEAST2, six trees were chosen at random. All trees were analysed with BEAST2 v.4.8 using the priors only mode (Bouckaert *et al.* 2014) and the sampled ancestors (SA) package (Gavryushkina *et al.* 2014). This analysis was run for 50 000 000 generations, sampling every 10 000 trees, yielding 5000 dated trees per run. Tracer v.1.7 showed convergence of runs and trees; effective sample size (ESS) values were >1000 and were subsequently summarized to produce a maximum credibility tree using TreeAnnotator v.2.4.8. The first 1000 trees (20%) of each run were discarded as burn-in. Node ages were extracted from the remaining trees using a script written by SSG (available in Groh *et al.* 2022, timescaling) and `ape` (Paradis & Schliep 2019) in R v.4.0.4 (R Core Team 2013).

Node age comparisons

There are two main reasons why we wished to compare node age estimates: (1) to understand the implications for neosuchian evolutionary history; and (2) to determine if there were any patterns in the results that the different methods delivered relative to each other and across different tree topologies. For the first aim, we determined the node age estimates for a series of 23 named nodes that potentially represent the origination of major clades within Neosuchia. Ages were extracted after all dating analyses, using the package ape (Paradis & Schliep 2019) in R v.4.0.4 (R Core Team 2013). The specified nodes are: Neosuchia (including Thalattosuchia); Neosuchia (excluding Thalattosuchia); Thalattosuchia; Tethysuchia; Dyrosauridae; Goniopholididae; Eusuchia; Crocodylia; Hylaeochampsidae; Gavialoidea; Gavialinae; Tomistominae; Brevirostres; Crocodyloidea; Crocodylidae; Mekosuchinae; Crocodylinae; Alligatoroidea; Alligatoridae; Alligatorinae; Diplocynodontinae; Globidonta; and Caimaninae. Most of the clade definitions follow Brochu (2003). Detailed definitions and the position of clades in our phylogenies can be found in Figures 2 and 3, and Groh *et al.* (2022, phylogenetics).

For the second aim (method comparison) we evaluated all nodes, not just the 23 named nodes mentioned above. We determined whether there was a statistically significant difference between the mean node age estimates, yielded by pairs of the dating methods, for a given node in a given tree topology. Thus, for example, for node X in topology Y, cal3 and EH would each provide 1000 node age estimates, and the means of these populations can then be compared using two-tailed *t*-tests (carried out here in Microsoft Excel 2021). This resulted in six two-tailed *t*-tests (cal3 compared to FBD, cal3 to EH, cal3 to sGLA, EH to FBD, EH to sGLA, FBD to sGLA) per node. If the *p*-value was significant (<0.05), we noted which method provided the younger and which method the older estimate.

RESULTS

Phylogenetic analysis

Our new phylogenetic analysis is based on the modified version of the Groh *et al.* (2020) dataset (see above) and yielded five MPTs (tree length = 276773.7 steps; Consistency Index (CI) = 0.222; Retention Index (RI) = 0.556) for the complete dataset (Fig. 2), and 41 MPTs (tree length = 248800; CI = 0.218; RI = 0.569) for the rediscretized dataset (Groh *et al.* 2022, phylogenetics). With the exception of Tethysuchia, all major neosuchian groups (Atoposauridae, Paralligatoridae, Aegyptosuchidae, Goniopholididae, Gavialoidea, Crocodyloidea, Tomistominae, Alligatoroidea, Diplocynodontinae) are recovered in our phylogenetic trees (Fig. 2; Groh *et al.* 2022, phylogenetics). Henceforth, we refer to the modified Groh *et al.* (2020) phylogeny as G21, and to the Stockdale & Benton (2021) phylogeny as SB21.

Comparison of different clade age estimation methods

The mean node age estimates and their standard deviations for each key clade highlight the differences between the four time-scaling methods used (Fig. 4). The results across all topologies from both sets of trees are very similar with only a few minor exceptions, which are detailed below.

Across all topologies, cal3 consistently delivers the statistically significantly youngest mean node age estimates for almost all nodes, compared to other methods (*p* < 0.05 for at least 99% of nodes compared to sGLA, 96.6% of nodes compared to EH and at least 66.7% compared to FBD). The only exceptions are nodes closer to the youngest tips, where FBD delivers significantly younger mean node age estimates than cal3. The oldest mean node age estimates are usually provided by EH, with at least 82.1% of all nodes having significantly older mean node age estimates than those produced by any other method. This pattern is only disrupted close to the root of the trees where sGLA and FBD often deliver the oldest ages. FBD and sGLA give relatively similar mean node age estimates, with 55–66% of mean node age estimates obtained by sGLA significantly older than those obtained by FBD and 4.3% of nodes showing no statistical difference in mean ages between the two methods (Groh *et al.* 2022, timescaling). These patterns apply to both the SB21 and G21 topologies.
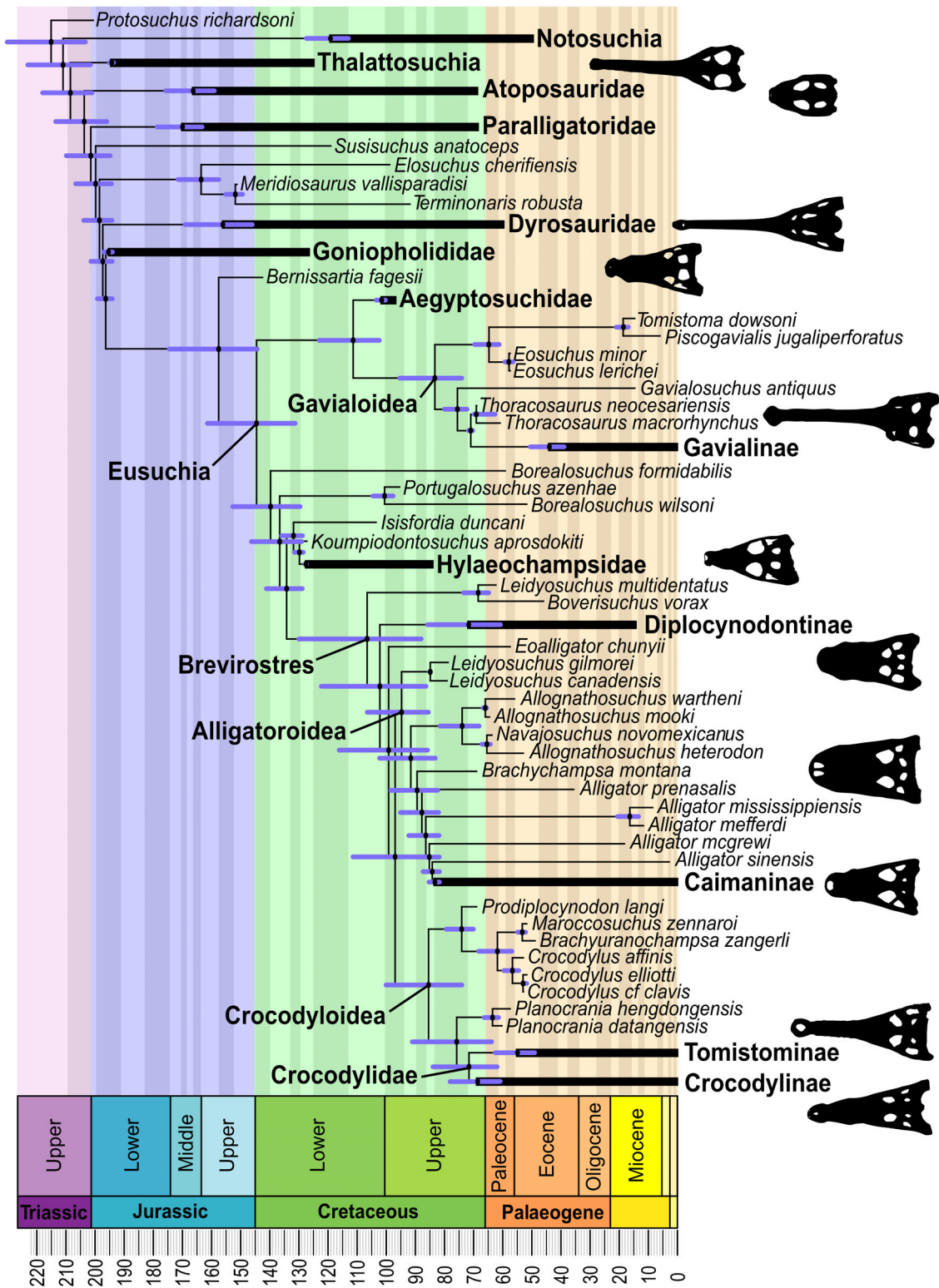
FIG. 2. Time-scaled phylogenetic tree of Neosuchia, based on Groh *et al.* (2020) with the modifications as set out in the text. The topology is the strict consensus tree based on the analysis of the complete dataset, after removal of the four rogue taxa. Node ages are scaled based on the mean ages of FBD and cal3 estimates and all MPTs. Horizontal purple lines represent the range of standard deviations between FBD and cal3 estimates.
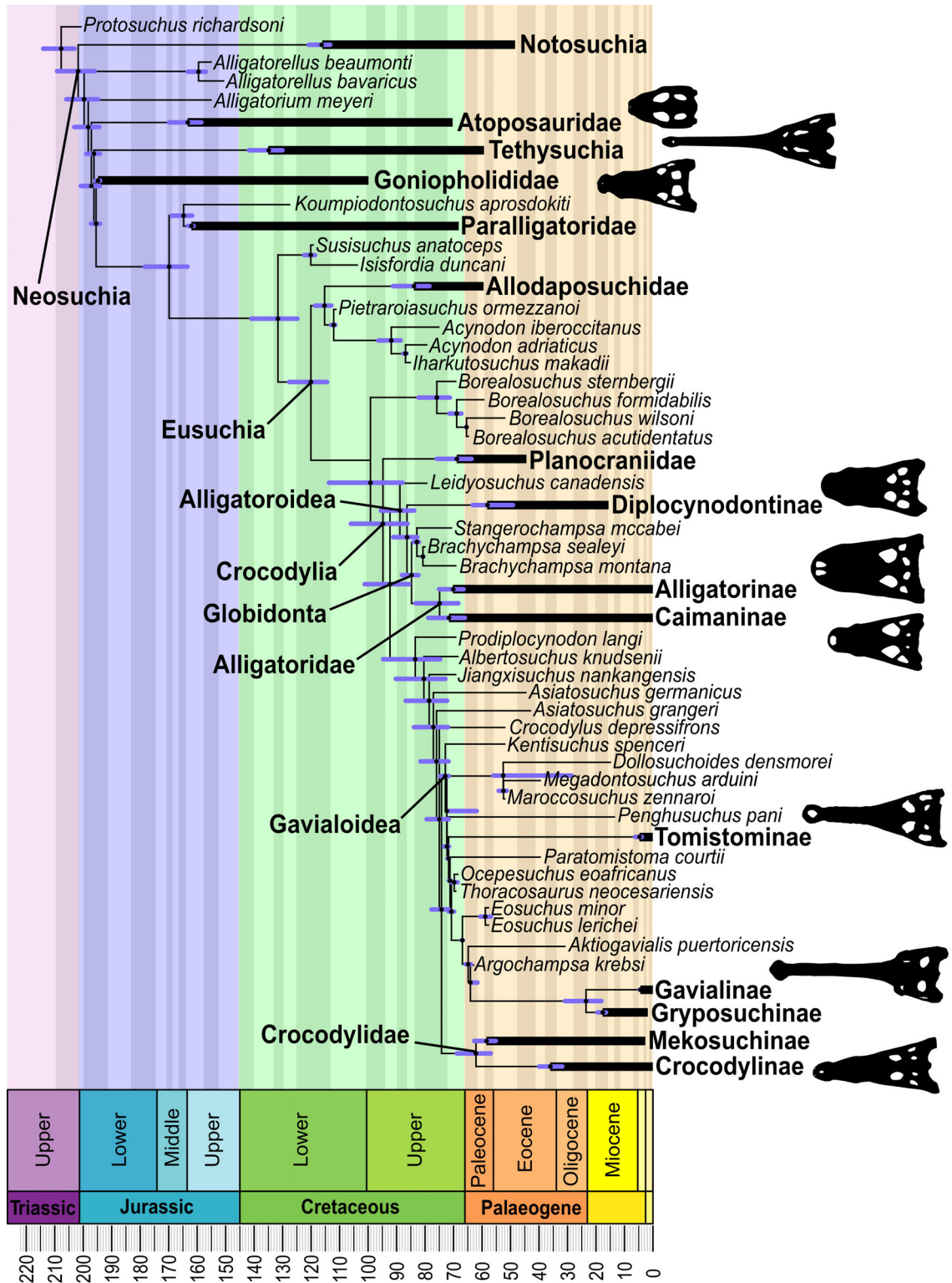
FIG. 3. Time-scaled phylogenetic tree of Neosuchia, based on Stockdale & Benton (2021). Note that species composition of clade terminals might differ to those in Figure 2. Node ages are scaled based on the mean ages of FBD and cal3 estimates and all MPTs. Horizontal purple lines represent the range of standard deviations between FBD and cal3 estimates.
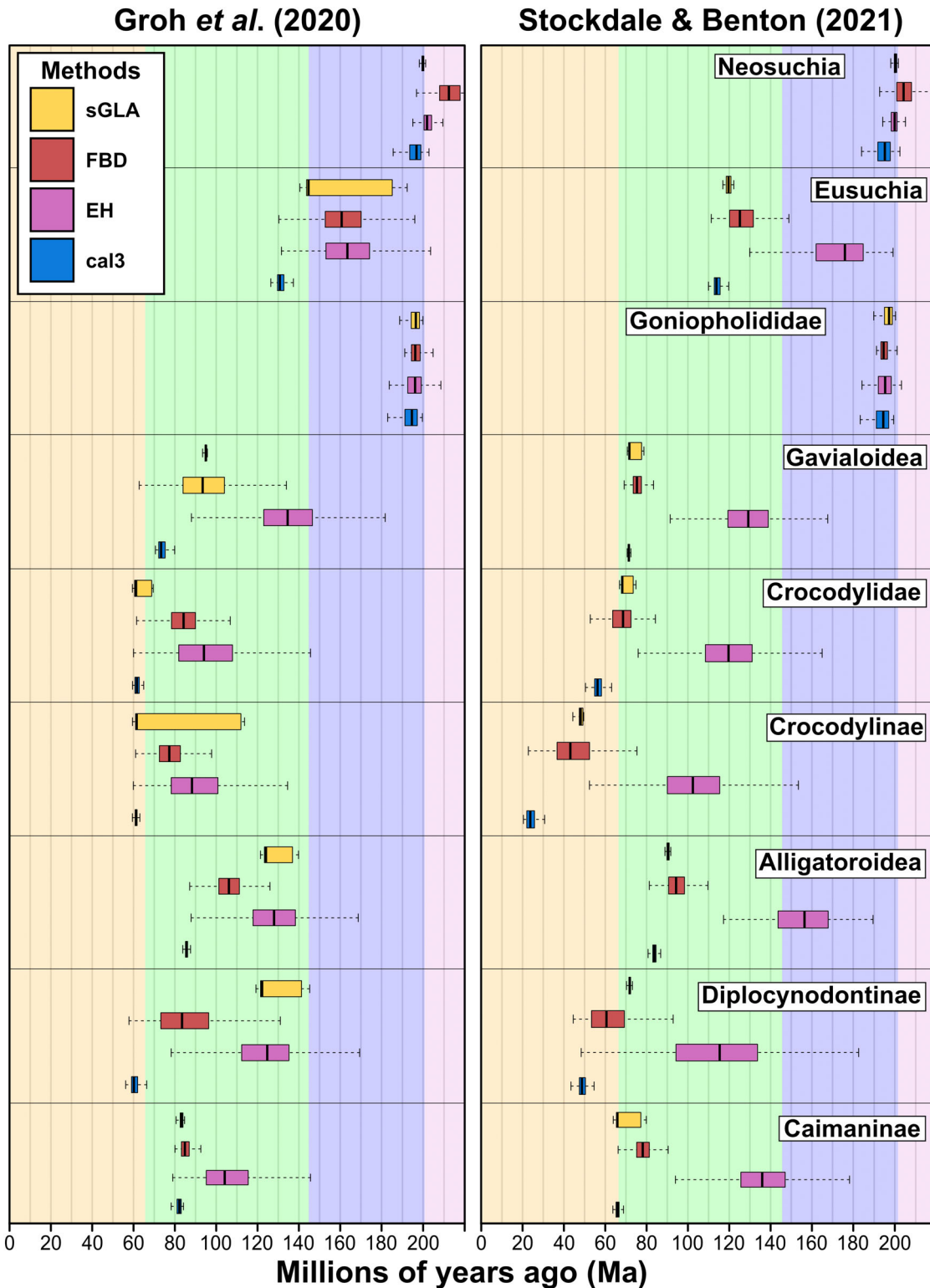
FIG. 4. Detailed origination time estimates for major neosuchian groups across the two different sets of phylogenies. The estimates based on our new phylogenetic analysis (modified from Groh *et al.* 2020) are derived from the analysis of the complete dataset, after removal of the four rogue taxa. The Stockdale & Benton (2021) estimates are based on their tree following the removal of Thalattosuchia. Plots show the median, upper and lower quartiles and range of estimates for each method.

The standard deviations of estimated node ages are usually low for cal3 and sGLA (always 10% or less than the total age estimate), intermediate for FBD (around 10%) and high for EH (usually above 10%). In addition, cal3 shows the lowest number of nodes that are influenced by the removal of the four rogue taxa in the G21 topologies, whereas EH, FBD and sGLA all experience great impact (Groh *et al.* 2022, timescaling). In the G21 topologies, removing the four rogue taxa leads to differences in mean node age estimates in five out of the twenty named clades, whereas mean ages were different for all named clades for FBD, and all but one (EH) and two named clades (sGLA) in the other two methods.

The variation in estimated clade ages increases with distance from the root, with a difference of 100% in several cases (e.g. Crocodylidae with mean node age estimates ranging from 62 Ma with cal3 to 127 Ma with EH in the G21 trees). In contrast, the difference in mean node age estimates close to the root is only 20% (e.g. Neosuchia with estimates ranging from 200.8 Ma (cal3) to 220.9 Ma (FBD)). A similar trend can be observed in the mean age estimates of unnamed nodes, with younger nodes closer to the tip showing a difference of up to 500% between youngest and oldest ages in several cases, whereas the difference is closer to 20–50% for older nodes closer to the root (Groh *et al.* 2022, timescaling).

For several nodes, the sGLA estimates display 'double peaks'. These bimodal distributions of age estimates do not denote differences in dating between tree topologies but occur for most crocodylian nodes in every tree, even when only a single topology is dated. We examine this anomaly in detail in the Discussion.

Origination times for key clades

Mean node age estimates for the origin of Neosuchia vary between 195 Ma (cal3) and 223 Ma (FBD) across all methods and both the G21 and SB21 phylogenies, with the majority of estimates between 200 and 205 Ma (Fig. 4). This clade age changes in only a minor way depending on whether Thalattosuchia is included in the definition of Neosuchia for both datasets (Table 4). Thalattosuchia is estimated to have originated between 193 Ma (FBD) and 203 Ma (EH) in the SB21 phylogeny.

Tethysuchia appears as two paraphyletic assemblages in both Groh *et al.* (2020) and G21 (Fig. 2). These two assemblages originate anywhere between 146 Ma (cal3) and 189 Ma (EH) for Dyrosauridae and 150 Ma (cal3) and 188 Ma (EH) for the clade consisting of *Elosuchus*, *Meridiosaurus* and *Terminonaris*, referred to as 'tethysuchian clade B' (TCB) henceforth, according to the full range of our analyses and topologies (Groh *et al.* 2022, timescaling). The G21 topology yielded clade ages of 146 Ma (cal3) to 184 Ma (EH) for Dyrosauridae (Table 4), and 157 Ma (cal3) to 184 Ma (EH/sGLA) for TCB respectively (Groh *et al.* 2022, timescaling). Results are markedly different for the SB21 phylogeny which includes a monophyletic Tethysuchia, with a different species composition compared to the G21 dataset. Depending on whether Thalattosuchia is included in Neosuchia, the estimated mean clade ages for Tethysuchia vary between 125 Ma (cal3) and 187 Ma (EH, with Thalattosuchia included). For Dyrosauridae in SB21, mean node age estimates fall between 73 Ma (cal3) and 150 Ma (EH, with Thalattosuchia included) (Table 4; Groh *et al.* 2022, timescaling). The mean node age estimates for Goniopholididae vary less markedly, between 194 Ma (cal3) and 197 Ma (FBD) for the G21 and 194 Ma (cal3) and 197 Ma (sGLA) for the SB21 trees (Figs 2–4; Table 4).

Origination time estimates for Eusuchia differ markedly, depending on whether or not the four rogue taxa are removed from the G21 tree. After taxon exclusion, mean node age estimates varied from 131 Ma (cal3) to 163 Ma (EH) for our preferred phylogeny (Table 4). Inclusion of the four taxa led to much older estimates in cal3 (144 Ma), FBD (177 Ma) and EH (171 Ma) (Groh *et al.* 2022, timescaling). For the SB21 topology, estimates varied between 114 Ma (cal3) and 175 Ma (EH, with Thalattosuchia included in Neosuchia) (Figs 2–4). The origination time estimates for Brevirostres (a clade not represented in SB21) are affected by taxon inclusion/exclusion in a similar way, with mean node age estimates derived from the G21 topology lying between 88 Ma (cal3) and 146 Ma (EH) after taxon exclusion and 143 Ma (cal3) and 156 Ma (EH) before exclusion (Groh *et al.* 2022, timescaling). Hylaeochampsidae (present only in the G21 tree) is estimated to have originated between 127 and 136 Ma by all four methods, irrespective of rogue taxon inclusion/exclusion (Fig. 2; Table 4).

Gavialoid mean clade age estimates are unaffected by the removal of the four rogue taxa from the G21 tree, ranging from 74 Ma (cal3) to 141 Ma (EH) across all trees and methods (Groh *et al.* 2022, timescaling), and 74 Ma (cal3) to 136 Ma (EH) for our preferred phylogeny (Table 4). Estimates for the SB21 tree are roughly similar, ranging from 71–76 Ma (cal3, sGLA, FBD) to 130 Ma (EH). Gavialinae (a clade not represented in SB21) shows an even wider proportionate variation in its node age estimates, from 39 Ma (cal3) to 92 Ma (EH) (Table 4).

Similar to Eusuchia, Crocodylia and Brevirostres, mean node age estimates for Crocodyloidea are influenced greatly by the presence of the four rogue taxa across all four methods for G21, and for Crocodylidae, Crocodylinae and Tomistominae across EH, sGLA and FBD. Crocodyloidea (not represented in SB21) is estimated as having originated between 74 Ma (cal3) and 117 Ma

TABLE 4. Summary of the different origination ages for the major neosuchian groups, as found by the four different methods for the two different topologies considered herein, excluding both rogue taxa and Thalattosuchia.

	Cal3		sGLA		FBD		EH	
	Groh *et al.*	Stockdale & Benton	Groh *et al.*	Stockdale & Benton	Groh *et al.*	Stockdale & Benton	Groh *et al.*	Stockdale & Benton
Neosuchia*	195.8 ± 3.7	194.5 ± 3.9	199.7 ± 0.6	200.2 ± 0.8	213.0 ± 7.8	204.9 ± 5.4	202.5 ± 4.2	204.5 ± 5.1
Tethysuchia		124.8 ± 2.5		150.8 ± 1.0		127.4 ± 8.1		175.4 ± 24.3
Dyrosauridae	145.9 ± 2.9	72.6 ± 1.2	183.5 ± 2.7	103.5 ± 2.0	168.4 ± 14.3	84.0 ± 8.3	180.5 ± 13.8	135.5 ± 18.8
Goniopholididae	193.9 ± 3.9	193.8 ± 3.9	196.2 ± 2.5	196.7 ± 2.4	196.6 ± 3.4	195.0 ± 2.5	195.5 ± 4.3	194.9 ± 7.6
Eusuchia	131.2 ± 2.7	114.2 ± 2.6	141.3 ± 1.1	119.4 ± 1.3	160.9 ± 12.2	126.6 ± 9.0	162.7 ± 14.4	173.7 ± 16.3
Hylaeochampsidae	127.3 ± 1.0	–	129.2 ± 1.4	–	127.8 ± 1.9	–	135.9 ± 11.3	–
Crocodylia	144.2 ± 2.9	85.4 ± 1.0	170.0 ± 1.2	95.7 ± 0.6	174.0 ± 14.0	100.5 ± 6.6	166.9 ± 15.5	163.3 ± 15.8
Gavialoidea	74.2 ± 2.8	71.4 ± 0.4	94.0 ± 0.5	73.5 ± 3.0	94.8 ± 15.1	75.7 ± 3.0	135.8 ± 17.4	129.6 ± 14.2
Gavialinae	39.2 ± 2.9	–	59.7 ± 0.4	–	50.4 ± 9.9	–	92.4 ± 23.3	–
Brevirostres	88.1 ± 2.7	–	122.4 ± 0.6	–	129.6 ± 9.3	–	146.0 ± 12.3	–
Crocodyloidea	74.1 ± 2.7	–	93.0 ± 0.3	–	99.8 ± 9.3	–	117.2 ± 16.9	–
Crocodylidae	62.0 ± 1.4	56.9 ± 3.1	64.9 ± 3.9	69.9 ± 2.8	83.7 ± 8.4	68.2 ± 5.9	95.1 ± 16.7	120.1 ± 14.8
Tomistominae	49.2 ± 3.1	–	59.0 ± 2.1	–	62.3 ± 10.6	–	59.6 ± 7.0	–
Mekosuchinae	–	55.1 ± 1.8	–	65.9 ± 2.1	–	62.2 ± 5.0	–	109.7 ± 20.1
Crocodylinae	61.3 ± 0.8	24.4 ± 2.8	64.2 ± 3.3	47.6 ± 1.1	77.8 ± 7.5	44.3 ± 10.4	90.3 ± 15.5	101.1 ± 22.8
Alligatoroidea	85.5 ± 0.7	83.6 ± 1.4	97.7 ± 0.5	90.3 ± 0.6	106.2 ± 7.0	94.7 ± 5.9	127.9 ± 15.0	158.8 ± 14.4
Diplocynodontinae	60.9 ± 2.8	49.2 ± 3.0	101.7 ± 0.4	71.7 ± 0.6	85.6 ± 15.8	62.0 ± 11.0	124.3 ± 19.5	111.7 ± 26.5
Alligatoridae	–	68.3 ± 2.9	–	78.3 ± 1.5	–	82.7 ± 4.6	–	144.6 ± 14.2
Alligatorinae	–	66.3 ± 1.4	–	73.9 ± 1.0	–	74.1 ± 5.8	–	140.9 ± 14.9
Globidonta	83.2 ± 1.5	82.1 ± 1.3	85.1 ± 0.6	83.6 ± 0.7	102.0 ± 6.4	87.3 ± 4.2	122.4 ± 16.1	149.3 ± 14.3
Caimaninae	81.8 ± 1.3	65.9 ± 1.4	83.0 ± 0.9	69.4 ± 6.0	85.2 ± 3.0	78.2 ± 4.5	107.3 ± 14.9	135.8 ± 12.9

Abbreviations: EH, extended Hedman; FBD, fossilized birth–death model; sGLA, smoothed ghost lineage analysis.
Results are based on the complete character set phylogeny, with the four rogue taxa removed from our new topologies (i.e. the modified Groh *et al.* (2020) dataset) and with Thalattosuchia excluded from the tree derived from Stockdale & Benton (2021).
*With Thalattosuchia excluded.

(EH) with rogue taxon exclusion (Table 4), and 143 Ma (cal3) to 153 Ma (EH) without taxon exclusion (Groh *et al.* 2022, timescaling). With respect to the G21 topology (with rogue taxon exclusion), the youngest estimates for the origination dates for Crocodylidae, Crocodylinae and Tomistominae are provided by cal3, at 62 Ma, 61 Ma and 49 Ma (Fig. 4; Table 4), respectively. The cal3 estimates remain the same, irrespective of taxon exclusion. EH provides the oldest age estimates for almost every clade: 95 Ma (Crocodylidae), 90 Ma (Crocodylinae) and 60 Ma (Tomistominae) with rogue taxon exclusion (Table 4) and 127 Ma (Crocodylidae) and 126 Ma (Crocodylinae) without (Groh *et al.* 2022, timescaling). The oldest mean age estimate for Tomistominae without taxon exclusion (78 Ma) is given by FBD. Tomistominae and Crocodyloidea cannot be accurately defined in the SB21 topology; however, this tree includes the crocodylid clade Mekosuchinae instead. The differences between the mean node age estimates found by the different methods for the same topologies are remarkable. Cal3 once again delivers the youngest estimates, of 57 Ma (Crocodylidae), 55 Ma (Mekosuchinae) and 24 Ma (Crocodylinae) for the topology without Thalattosuchia (Table 4), with very similar ages if Thalattosuchia is included in Neosuchia. EH provides the oldest ages: 120 Ma (Crocodylidae), 110 Ma (Mekosuchinae) and 101 Ma (Crocodylinae). FBD and sGLA ages are very similar, ranging between 68 and 70 Ma (Crocodylidae), 62–66 Ma (Mekosuchinae) and 44–48 Ma (Crocodylinae) (Table 4).

Whereas the cal3 mean node age estimates of Alligatoroidea, Diplocynodontinae, Globidonta and Caimaninae vary only slightly between different methods, rogue taxon exclusion strongly influences the mean node age estimates provided by EH, FBD and sGLA for the G21 topology. Cal3 provides the youngest estimates for all four groups, with clade ages of 86 Ma (Alligatoroidea), 61 Ma (Diplocynodontinae), 83 Ma (Globidonta) and 82 Ma (Caimaninae) (Table 4). Ages given by EH consistently prove to be the oldest estimates across all topologies: 128 Ma (Alligatoroidea), 124 Ma (Diplocynodontinae), 122 Ma (Globidonta) and 107 Ma (Caimaninae) with rogue taxon exclusion (Table 4), and 140 Ma (Alligatoroidea), 138 Ma (Diplocynodontinae), 136 Ma (Globidonta) and 110 Ma (Caimaninae) without taxon exclusion (Groh *et al.* 2022, timescaling).

Excluding Thalattosuchia from Neosuchia has little influence on the mean clade age estimates obtained from the SB21 topology. In addition to the groups found in the G21 tree, the SB21 topology also includes the clades Alligatoridae and Alligatorinae. As for G21, cal3 provides the youngest estimates for the SB21 tree: 84 Ma (Alligatoroidea), 82 Ma (Globidonta), 49 Ma (Diplocynodontinae), 68 Ma (Alligatoridae), 66 Ma (Alligatorinae) and 66 Ma (Caimaninae) (Table 4). FBD and sGLA ages are

approximately 10–20 myr older than those obtained with cal3, whereas EH once again delivers the oldest estimates: 159 Ma (Alligatoroidea), 150 Ma (Globidonta), 112 Ma (Diplocynodontinae), 145 Ma (Alligatoridae), 141 Ma (Alligatorinae) and 136 Ma (Caimaninae) (Table 4).

DISCUSSION

Neosuchian phylogeny

Modifying the dataset of Groh *et al.* (2020) resulted in similar tree topologies to those recovered by that study, with a few noteworthy differences. Depending on whether Thalattosuchia is considered a neosuchian (Pol & Gasparini 2009; Bronzati *et al.* 2012; Adams 2014) or non-neosuchian mesoeucrocodylian (Wu *et al.* 2001*b*; Young & Andrade 2009; Holliday & Gardner 2012) clade, its position in our phylogenies can be described as the sister group to all other neosuchians, or the closest outgroup to Neosuchia (Fig. 2). Paralligatoridae and Atoposauridae have clustered together in some previous studies (Rogers 2003; Turner & Pritchard 2015; Schwarz *et al.* 2017), but have been placed in a variety of different positions in others, such as either the closest sister group to Eusuchia (Adams 2014) or part of Eusuchia (Turner 2015; Turner & Pritchard 2015; Schwarz *et al.* 2017). In the G21 trees where continuous characters are treated as such, they constitute the two earliest diverging neosuchian clades (apart from Thalattosuchia, if the latter is included in Neosuchia). In the rediscretized analysis, Paralligatoridae and Atoposauridae are resolved as sister groups (Groh *et al.* 2022, phylogenetics), similar to the results in Rogers (2003).

Groh *et al.* (2020) found a paraphyletic Tethysuchia, in contrast to several earlier studies (Hastings *et al.* 2010; Andrade *et al.* 2011; Puértolas *et al.* 2011; Martin *et al.* 2016). Our G21 results also identify Tethysuchia as paraphyletic, with *Elosuchus* and the newly added *Meridiosaurus* forming a sister group to Dyrosauridae and the remaining neosuchians. *Elosuchus* and *Meridiosaurus* are grouped together on the basis of several continuous characters, as well as the presence of two discrete apomorphies (a dorsally broad postorbital bar (char. 211) and long squamosal prongs (char. 231)). Our Dyrosauridae, which is similar in species composition to the group supported by Martin *et al.* (2016), is not clearly resolved, and is characterized by a five taxon polytomy in the consensus tree in both analyses. *Susisuchus anatoceps* is no longer placed as part of Goniopholididae as it was in Groh *et al.* (2020), but instead is found as a non-eusuchian neosuchian that occupies varying positions, because of the addition of atoposaurids, paralligatoroids and *Calsoyasuchus* to the dataset. Goniopholididae now

includes *Vectisuchus* and both species of *Sunosuchus*, because of the absence of *Susisuchus* as part of the clade. Goniopholidid monophyly is based on the quadratojugal-jugal suture lying at the posterior angle of the infratemporal fenestra (char. 264); the vomer being exposed on the palate between the palatines (char. 346); the flat lateroventral surface of the dentary anterior to the external mandibular fenestra (char. 401); and thick and vertical osteoderm margins (char. 551).

Bernissartia fagesii forms the closest sister group to Eusuchia, a similar result to that found by previous analyses (Sweetman *et al.* 2014). Aegyptosuchidae has previously been placed as the sister group to Brevirostres (Delfino *et al.* 2008) or in a polytomy with Gavialoidea (Sereno & Larsson 2009; Holliday & Gardner 2012). Our analyses support and clarify the latter proposal, with Aegyptosuchidae and Gavialoidea being sister taxa, and this clade diverging from the remaining eusuchians. Aegyptosuchidae and Gaviaoidea are united by: the absence of a wide frontal plate in the anteromedial corner of the supratemporal fenestra (char. 193); the frontoparietal suture making a modest entry into the supratemporal fenestra (char. 194); long squamosal prongs, covering at least 10% of the paroccipital process (char. 231); and the presence of the parietopostorbital suture within the supratemporal fenestra (char. 243). Hylaeochampsidae is usually resolved as a non-crocodylian eusuchian family (Andrade *et al.* 2011; Puértolas-Pascual *et al.* 2014; Narváez *et al.* 2015). Our results, however, consistently place it as the sister group to Brevirostres, similar to Groh *et al.* (2020), together with the newly added bernissartiid *Koumpiodontosuchus aprosdokiti* (Sweetman *et al.* 2014) and the susisuchid *Isisfordia duncani* (Salisbury *et al.* 2006), a placement that was explored in more detail in Groh *et al.* (2020).

Previous work has placed Diplocynodontinae within Alligatoroidea (Brochu 1999; Delfino & Smith 2012), whereas our results resolve it as the sister group to the remaining Brevirostres. As previously found by Groh *et al.* (2020), Alligatorinae remains paraphyletic (Fig. 2). Both issues have been discussed in detail in the former publication. Thus far, members of the genus *Brachychampsa* have been recognized as early alligatoroids (Pinheiro *et al.* 2013; Bona *et al.* 2018; Massonne *et al.* 2019). However, our results group the newly added *Brachychampsa sealyi* (Williamson 1996), argued to be a valid taxon by Brochu (2004), with Caimaninae, based on the existence of a lateral process of the palatines projecting into the suborbital fenestra on the anterior lateral edge (char. 364).

As mentioned above and found in previous studies such as Salisbury *et al.* (2006), Puértolas *et al.* (2011) and Groh *et al.* (2020), Crocodyloidea is divided into three major clades: early diverging Crocodyloidea, Tomistominae and Crocodylinae. Planocraniidae, which is usually resolved as an early diverging eusuchian family (Pol *et al.* 2009; Puértolas *et al.* 2011; Brochu 2012; Holliday & Gardner 2012), is placed as an early crocodyloid clade by the G21 analyses, as in Groh *et al.* (2020).

Comparison of methodological results

Cal3 generally delivered the youngest age estimates in this study, with the lowest standard deviations of all methods. These low standard deviations rarely encompassed the age ranges given by the other methods. Moreover, the deletion of taxa had a much lower impact on cal3 node ages compared to the other three methods. Indeed, cal3 estimates often remained similar despite differences in the tree topologies analysed: for the G21 dataset, mean node age estimates for the discrete and complete character set based topologies were the same for many nodes (Groh *et al.* 2022, timescaling); for the SB21 dataset, mean node age estimates were the same or within 2 myr of each other for all nodes (except those within Tethysuchia), irrespective of whether or not Thalattosuchia was removed from Neosuchia (Groh *et al.* 2022, timescaling).

Knowing how the four different methods work and the assumptions they make can help us to understand the above results. Cal3 initially sets the youngest possible age for a node as the first appearance date (FAD) of the oldest member of the clade that is to be dated. It then determines the probability distribution of the potential node ages by moving from root to shallowest node from this point onwards, using pre-determined extinction, speciation and sampling rates (Bapst 2013). However, determining these rates can be more difficult in the presence of a large number of singleton taxa (Bapst 2013, 2014). In addition, a number of branches exhibited the minimum branch length of 0.1 myr (set in accordance with the recommendations of Bapst 2014), which potentially introduces an arbitrary component to the results. Because cal3 bases its initial node age estimate on the oldest age within a clade, rather than its closest relatives, the tendency of cal3 to produce the youngest age estimates is to some extent an artefact of how the method works. However, the other methods have similar artefacts that lead, for example, to much older estimates (EH).

There are two types of taxon removal that can impact age estimates: (1) general taxon exclusion/absence; and (2) absence/exclusion of the oldest taxon in a clade. Cal3 is particularly sensitive to the second type of taxon removal, because the oldest taxon within the clade plays a critical role in determining the other node age estimates. This is exemplified by the case of Crocodyloidea in the G21 topologies, with mean node age estimates of 142.5 Ma (before the removal of *Susisuchus jaguaribensis*)

and 74.1 Ma (after removal). Estimates can be shifted strongly towards younger node ages if the oldest known taxon is missing. However, cal3's estimation method is also the reason for its robustness concerning other changes in tree topology, such as the general removal of individual taxa (as long as they are not the oldest in a clade) and minor rearrangements of more deeply nested taxon interrelationships. Similarly, the removal of entire taxon groups, such as Thalattosuchia in the SB21 topology, has little effect on downstream ages when cal3 is applied, with differences of 100 000 years or less in the mean ages of the main nodes. If the order of taxa within a clade changes slightly, the overall initial minimum clade age tends to remain the same.

The results of EH stand in stark contrast to those of cal3. For the majority of nodes, it provides the oldest mean node age estimates, sometimes more than twice as old as those of cal3 (e.g. Gavialinae in G21). This effect is even more pronounced for the SB21 topologies, with EH mean age estimates often twice as old as the ones obtained by cal3, and up to four times as old (e.g. for Crocodylinae). In addition, EH standard deviation rates increase with distance from the root in both sets of topologies and are considerably larger, often 3–10 times higher than those of cal3, with minimum and maximum age estimates spanning a much wider range (Fig. 4). These SD ranges partially encompass the ranges of the other age estimates, overlapping with the cal3 means 33% of the time, with FBD estimates 61% of the time, and with sGLA estimates 63% of the time, for the G21 topology (Groh *et al.* 2022, timescaling). Although they did not report markedly younger cal3 estimates, similarly high standard deviations for EH were observed by Lloyd *et al.* (2016) in their study of dinosaurs. In contrast to Lloyd *et al.* (2016), however, our analyses found that altering the ages of the additional outgroups had little influence on the obtained estimates.

EH estimates are based on the taxon ages within successive outgroups to the clade that is being dated. This dependence on the taxa contained within more than one clade produces a higher sensitivity to changes in tree topology, especially further from the root of the tree. These changes include both general taxon exclusion/absence and removal of the oldest taxon in a clade. It also makes the method particularly sensitive to sampling issues and biases. If a clade is part of a well-sampled group with multiple species in each time bin, EH will produce younger age estimates that are closer to those of cal3, as observed previously (Lloyd *et al.* 2016). By contrast, the older the ages for the 'successive outgroups' to the dated clades, the older the obtained node ages. For the G21 topologies, this effect is demonstrated by Caimaininae (ages of 81.8 Ma and 107.3 Ma yielded by cal3 and EH, respectively) and Gavialoidea (ages of 74.2 Ma and

135.8 Ma yielded by cal3 and EH, respectively). Although poorer taxon sampling is likely to increase errors when applying any origination time estimation method, EH seems to be particularly influenced by both lower taxon coverage and uneven sampling of the fossil record.

In most cases, and for both sets of topologies, FBD supplied node ages younger than those given by EH and older than those obtained from cal3. The exceptions are the nodes closest to the root, where FBD estimates were the oldest of those provided by any method. FBD age estimates display intermediate standard deviations between the low and high values obtained by cal3 and EH, respectively. The ranges of the FBD age estimates often overlap with those from EH (although there is still a statistically significant difference in means: Fig. 4). FBD calculates node ages by using priors to determine the evolutionary rates along the entire tree. These rates are changeable throughout different time intervals, as per the skyline version of FBD (Gavryushkina *et al.* 2014). Although FBD does not rely on the ages of single taxa within clades for minimum node age estimates, unlike cal3 and EH, it was even more strongly influenced by the removal of the four rogue taxa than the former two methods. This includes both exclusion of the oldest taxon in a clade, and the general removal of taxa. By contrast, minor differences in tree topology cause less variation in node age estimates than they do in cal3.

FBD assumes constant speciation, extinction and sampling rates among phylogenetic branches over time and, accordingly, scales node ages even of successive older nodes, as can be seen with the estimates for the nodes close to the tree root. For example, whereas cal3, EH and sGLA suggest a diversification burst in early-branching neosuchians and closely related sister groups shortly after the end of the Triassic, FBD postulates a Late Triassic origin for Neosuchia for both sets of topologies, with a much more substantial amount of time passing between each node in the tree (Groh *et al.* 2022, timescaling). On average, there is less than a million years between the earliest neosuchian nodes in cal3: by contrast, the nodes in the phylogeny time-scaled with FBD are, on average, at least 2 myr apart.

The estimates obtained by sGLA display variable relationships with those produced by the other three methods. Estimates for nodes close to the root tend to be older, whereas more tipward node age estimates are younger and, at times, approach those of cal3. For both the G21 and SB21 topologies, sGLA mean node age estimates are usually similar to those from FBD, both in mean age and standard deviations. This is in contrast to previous studies, which found sGLA ages to be older than those obtained by FBD (Turner *et al.* 2017). As in EH, sGLA uses the next closest outgroup to the node being dated to establish a minimum node age. However, instead

of taking multiple 'successive' outgroups into account, it relies only on the closest sister group in establishing the minimum age and scales up the estimate in accordance with the age of earlier nodes.

Our results show that sGLA is the method most sensitive to the general exclusion of single taxa (including the oldest one within a clade), although it does not respond as strongly to minor changes in topology as EH. Because sGLA adjusts node age estimates based on older taxa, it shares EH's greater sensitivity to sampling bias and coverage. Unlike cal3 and EH, sGLA is not per se a stochastic time-scaling algorithm, as can be seen in the anomalously bimodal frequency distribution of sGLA node age estimates. We have been unable to find an exact source for these bimodal distributions, as a detailed exploration of the mathematical background of the method lies beyond the scope of this paper.

Finally, it is often argued that greater taxon sampling (facilitated by the use of supertrees) is preferable when investigating a group's macroevolutionary history (e.g. Haeseler 2012). Here, the application of four dating methods to two independent sets of topologies with different levels of taxon sampling, allows us to examine this issue with regard to the best practice for establishing node ages. The different methods deliver roughly similar results using either the G21 MPTs or the SB21 supertrees; EH delivers the oldest mean node age estimates, and cal3 the youngest. As stated above, some methods (such as EH) are more influenced by poor taxonomic coverage than others, so the use of more taxon-rich supertrees might be regarded as preferable. However, our analyses demonstrate that the stratigraphic position of the sampled taxa is more important than overall taxonomic coverage. Specifically, the inclusion of the oldest taxon for each clade is paramount, because many methods determine node ages by using the oldest taxon within, or closely related to, the clades whose age is to be estimated. This phenomenon is illustrated by the G21 estimates for Crocodylinae, Diplocynodontinae and Eusuchia. All three groups were assigned unrealistically young clade ages (as judged from the fossil record) in the SB21 topology because of the omission of the oldest known fossils. In other cases, the greater taxon sampling of the SB21 supertree proved advantageous, delivering more stratigraphically consistent age estimates (e.g. for Dyrosauridae and Tethysuchia; see below).

Recommendations

Previous studies have advocated the use of stochastic time-scaling approaches such as cal3 and EH, over simpler methods like sGLA (Lloyd *et al.* 2016; Bapst & Hopkins 2017), as well as emphasizing the importance of complete taxon sampling (Lloyd *et al.* 2016) and the role of cal3 as a viable alternative to FBD (Bapst *et al.* 2016). They have also recommended the use of EH for groups with low sampling rates, and the use of cal3 for those with high sampling rates (Soul & Friedman 2017), as well as the theory underlying FBD (Bapst 2013). Other studies have used cal3, sGLA and EH to date trees for analyses of trait evolution, such as body mass in Dinosauria and Crocodylomorpha (Benson *et al.* 2018; Godoy *et al.* 2019), and extinction as a binary trait in non-teleostean actinopterygians, end-Permian tetrapods and archosauromorphs (Puttick *et al.* 2017; Soul & Friedman 2017; Allen *et al.* 2019). None of these studies, however, discussed the differences in estimated node ages themselves, only their impact on model selection and trait evolution coefficients.

After evaluating all four methods, we propose some recommendations for the best way of estimating clade ages in future studies.

1. It is clear that the various time-scaling methods produce different (often radically different) results. As such, it is dangerous to pick one method, apply it and take the results at face value, because this would not account for any sensitivity to the choice of method that the results might display. Applying only a single method could lead to an incomplete sampling of possible node ages and heavily skew estimates. If only one method is to be applied, then this choice should be justified based on the properties of the dataset (e.g. proportion of singletons, the extent of coverage of the earliest clade members, overall taxon sampling). Ideally, however, multiple dating methods should be applied (see Recommendation 5, below). If the latter leads to unhelpfully wide ranges for particular nodes of interest, then narrower 'preferred' node ages may be justified based on the results of the method(s) that appears best suited to the properties of the dataset.

2. Although taxon sampling as a whole is important, studies should pay special attention to the inclusion of the oldest putative members of the clades they wish to date. Without the inclusion of these species, mean node age estimates are often too young, even if the taxonomic coverage is otherwise good; as when supertrees are used, for example.

3. Extended Hedman generally yields older dates that often imply longer ghost ranges than the other methods, such as the 105 myr-long ghost range leading to *Borealosuchus formidabilis* in the G21 topology, compared with the 70 myr identified by cal3 and FBD (Groh *et al.* 2022, timescaling). The most significant problem is EH's sensitivity to various different issues, such as taxon absence/removal and sampling bias. It should thus only be applied to datasets with

high taxon sampling for all the known clades within a tree but should be considered for use as an alternative to cal3 in the presence of numerous singletons. However, when doing so, particular attention should be paid to issues of tree topology and taxon sampling.

4. sGLA is the single most sensitive method to taxon exclusion and does not include stochastic estimates and is thus unsuitable for most analyses. In addition, the artefactually bimodal distributions for its age estimates make a correct age estimation difficult, especially in the presence of extant taxa.

5. We recommend the use of both cal3 and FBD for most datasets, especially those with incomplete taxon sampling. Care should be taken, however, when using methods such as cal3 that rely on prior estimation of speciation, extinction and sampling rates without phylogenetic information on datasets with a high proportion of singletons.

Clade ages and neosuchian evolutionary history

Below, we place our estimated clade ages in the wider context of previous work and consider their implications for understanding neosuchian evolution. Previous studies have estimated the origination time for Neosuchia as between 189 and 209 Ma (Andrade *et al.* 2011; Turner *et al.* 2017; Godoy *et al.* 2019; Table 1), or more generally as Late Triassic to Early Jurassic (Pol *et al.* 2009; Montefeltro *et al.* 2013). The ages found for both the G21 and SB21 topologies (both with and without Thalattosuchia included) agree with these ranges (Figs 2–4; Table 4), with only FBD yielding slightly older ages of up to 217 Ma.

A substantial amount of early neosuchian diversification took place during the Early Jurassic. All four methods agree that for the G21 trees, the lineages leading to Tethysuchia, Goniopholididae, Paralligatoridae, Atoposauridae and Eusuchia had diverged from each other by 180 Ma (Fig. 2). The clade ages based on the SB21 phylogeny agree, with the exception of the lineage leading to Paralligatoridae, which is estimated to have diverged during the Middle Jurassic (Fig. 3). With regard to stem-eusuchian lineages and Eusuchia, our two preferred methods (cal3 and FBD) suggest two different evolutionary histories based on both the G21 and SB21 phylogenies (Table 4): (1) rapid divergence of the remaining non-eusuchian neosuchian clades from the main lineage leading to Eusuchia during the Early Jurassic, between 190–200 Ma (cal3, also supported by sGLA); or (2) a slower diversification during the Late Triassic and Early Jurassic, 190–220 Ma (FBD, also supported by EH). We favour the scenario of a rapid early burst of diversification during the earliest Jurassic supported by cal3 (and sGLA) for both sets of topologies, because it coincides with the increased availability of ecological niches following the end-Triassic mass extinction (see below).

Previous node-based origination time estimates for a monophyletic Tethysuchia have ranged across the Early–Middle (Turner *et al.* 2017; Godoy *et al.* 2019) or Late (Martin *et al.* 2010; Andrade *et al.* 2011) Jurassic (Table 1). In the G21 topologies, Tethysuchia forms two separate clades (Dyrosauridae and tethysuchian clade B (TCB)), although their origination dates do not differ substantially from each other. Cal3 and FBD corroborate a Middle–Late Jurassic origin for Dyrosauridae, with ages of 146 Ma (cal3) and 168 Ma (FBD), and ages of 157 Ma (cal3) to 171 Ma (FBD) for TCB. For Dyrosauridae, this implies a very long ghost range of over 70 myr. In contrast to the G21 trees, the SB21 topology includes a monophyletic Tethysuchia, leading to substantially different mean clade age estimates. It places the origin of Tethysuchia in the Early Cretaceous, 125 Ma (cal3) to 135 Ma (FBD), irrespective of whether or not Thalattosuchia is included in Neosuchia. Using SB21, Dyrosauridae is estimated to have originated during the Campanian, 73 Ma (cal3) to 84 Ma (FBD), eliminating the ghost range found in the G21 topology and providing a more stratigraphically consistent age estimate (Fig. 3). We favour the Middle to Late Jurassic tethysuchian origin dates based on the environmental changes discussed below and the stratigraphically more consistent Campanian dates for Dyrosauridae provided by the SB21 topologies.

Despite diverging from other neosuchians later than Tethysuchia, Goniopholididae is currently known from some records that appear earlier in the fossil record. The earliest putative goniopholidid, *Calsoyasuchus valliceps*, is known from the Early Jurassic, over 190 Ma (Tykoski *et al.* 2002; Andrade *et al.* 2011), although one recent study placed it outside Neosuchia (Wilberg *et al.* 2019). In line with the estimates of 184–197 Ma proposed by previous studies (Andrade *et al.* 2011; Turner *et al.* 2017; Godoy *et al.* 2019; Table 1), our analyses estimate an Early Jurassic origination date for Goniopholididae, between 194–197 Ma for both the G21 and SB21 topologies, as part of the wider increase in crocodylomorph diversity after the end-Triassic extinction. The core group of youngest goniopholidids, *Goniopholis*, *Amphicotylus* and *Anteophthalmosuchus*, has previously been estimated to have originated 147–160 Ma (Andrade *et al.* 2011; Turner *et al.* 2017; Godoy *et al.* 2019). Our cal3 and FBD estimates for the G21 topologies are slightly older, ranging from 153–171 Ma.

Both Late Jurassic (Andrade *et al.* 2011; Turner *et al.* 2017; Mateus *et al.* 2018) and Early Cretaceous (Salisbury *et al.* 2006; Pol *et al.* 2009; Martin *et al.* 2010; Puértolas *et al.* 2011; Lee & Yates 2018; Godoy *et al.* 2019) origins for Eusuchia have been proposed (Table 1). Our two

favoured origination time estimation methods each support one of these possibilities for the G21 topology, yielding origination dates from 131 Ma (cal3) to 161 Ma (FBD). Similar to the pattern observed for the neosuchian origination date, the two suggested evolutionary scenarios for the main eusuchian clades are either gradual (FBD) or with several diversification bursts over a shorter time period (cal3). If *Susisuchus jaguaribensis*, a susisuchid or early neosuchian (Fortier & Schultz 2009; Turner & Pritchard 2015), is included as an early crocodyloid, these ages are skewed substantially towards older, Late Jurassic estimates. The mean node age estimates obtained for the SB21 topology are younger, ranging from 114 Ma (cal3) to 127 Ma (FBD). This is mainly because of the omission of the oldest known eusuchian, the Barremian *Hylaeochampsa vectiana* (Clark & Norell 1992), from the SB21 supertree, leading to unrealistically young estimates for the eusuchian clade age (Fig. 3). Therefore, we favour the scenario proposed by the G21 cal3 estimates, placing the origin of Eusuchia shortly after the Jurassic–Cretaceous boundary (Fig. 5).

In contrast to Eusuchia, crocodylian origination ages have mostly been estimated as Late Cretaceous (Salisbury *et al.* 2006; Roos *et al.* 2007; Martin *et al.* 2010; Andrade *et al.* 2011; Oaks 2011; Puértolas *et al.* 2011; Turner *et al.* 2017; Lee & Yates 2018; Solórzano *et al.* 2019), with one Early Cretaceous exception (Godoy *et al.* 2019) (Table 1). Dates based on the G21 dataset have been estimated as slightly earlier because of the inclusion of Hylaeochampsidae and Aegyptosuchidae as crocodylian clades (Fig. 2). As a result of the way the clade name definitions for Eusuchia and Crocodylia map onto the G21 topologies, these two clades are identical and so have a single ancestral node and clade age estimate. The most likely origin date for this G21 Eusuchia–Crocodylia clade is Late Jurassic or Early Cretaceous. Early Cretaceous origination time estimates for Crocodylia, however, have been strengthened recently by the discovery of *Portugalosuchus azenhae*, a potential crocodylian from the Cenomanian (Mateus *et al.* 2018), which is included in the G21 phylogeny. The SB21 topology does not include *Portugalosuchus* or *Hylaeochampsa*, and thus produces much younger and less likely mean node age estimates, of 85 Ma (cal3) to 101 Ma (FBD). In short, an Early Cretaceous origin of Crocodylia is most likely.

Similar to Crocodylia, Late Cretaceous clade ages have also been suggested for Brevirostres (Salisbury *et al.* 2006; Martin *et al.* 2010; Puértolas *et al.* 2011; Turner *et al.* 2017). The oldest possible specimen referable to Brevirostres (as well as Crocodyloidea, Crocodylidae and Crocodylinae) is hard to determine because of the ambiguous status of many fossils labelled as 'Crocodylus', with many relevant specimens either not belonging to Crocodylinae or being very fragmentary (Brochu 2000; Oaks 2011). For example, incomplete mandible fragments from the Cenomanian, described as *Crocodylus selaslophensis* (Molnar & Willis 2001), have recently been re-identified as belonging to the susisuchid *Isisfordia* (Hart *et al.* 2019; Hart 2020). As with Eusuchia, FBD and cal3 mean node age estimates differ substantially in the G21 topology, suggesting either: (1) a date of 87 Ma for Brevirostres (cal3) and a late Early to Late Cretaceous diversification of the main eusuchian groups (Gavialoidea, Hylaeochampsidae, Brevirostres); or (2) a date of 130 Ma for Brevirostres and a more gradual evolution of these clades mostly during the Early Cretaceous (FBD) (Fig. 5). In contrast to the G21 trees, the clade definition of Brevirostres means that the latter includes Gavialoidea in the SB21 topology, with clade age estimates for the group placed during the Late Cretaceous, similar to the cal3 estimates for the G21 dataset. It is difficult to prefer one of these two scenarios, because both can be linked to biotic and abiotic factors that might have promoted diversification (see below).

The diversification of Eusuchia during the Late Cretaceous included the origin of Gavialoidea, which occurred between 71 and 90 Ma, according to earlier studies (Salisbury *et al.* 2006; Martin *et al.* 2010; Puértolas *et al.* 2011; Brochu 2012; Turner *et al.* 2017; Godoy *et al.* 2019; Table 1). This is in line with the mean node age estimates we obtained with our preferred methods, cal3 and FBD, for both the G21 and the SB21 datasets, with ages varying from 71 Ma (cal3) to 95 Ma (FBD). EH estimates are substantially older for both sets of topologies and Early Cretaceous in age (Table 3), a discrepancy that persists throughout the gavialoid part of the tree, as far as Gavialinae. Cal3 and FBD place the origin of Gavialinae after the K/Pg boundary, at 40 Ma and 50 Ma, respectively (Fig. 2). Therefore, a Late Cretaceous origin of Gavialoidea is likely, as is an early Palaeogene origin of Gavialinae, potentially promoted by abiotic factors (see below).

Establishing a firm minimum clade age for Crocodyloidea is difficult because of the above mentioned problem with the accurate identification of early 'Crocodylus' species, but most previous morphological studies suggest similar middle–Late Cretaceous origination dates (Salisbury *et al.* 2006; Martin *et al.* 2010; Puértolas *et al.* 2011; Lee & Yates 2018; Mateus *et al.* 2018; Godoy *et al.* 2019). Our estimates for the G21 topology (there is no direct equivalent to Crocodyloidea in SB21) are strongly influenced by the presence of *Susisuchus jaguaribensis*. Removing it from the phylogeny leads to middle (100 Ma, FBD) or Late Cretaceous (74 Ma, cal3) dates for the origin of the crocodyloid clade (Figs 2, 4).

The current literature is divided on whether Crocodylidae was present before the K/Pg boundary (Table 1). Some studies argue for a Late Cretaceous origin of the clade (Brochu 2003; Martin & Delfino 2010; Martin *et al.*
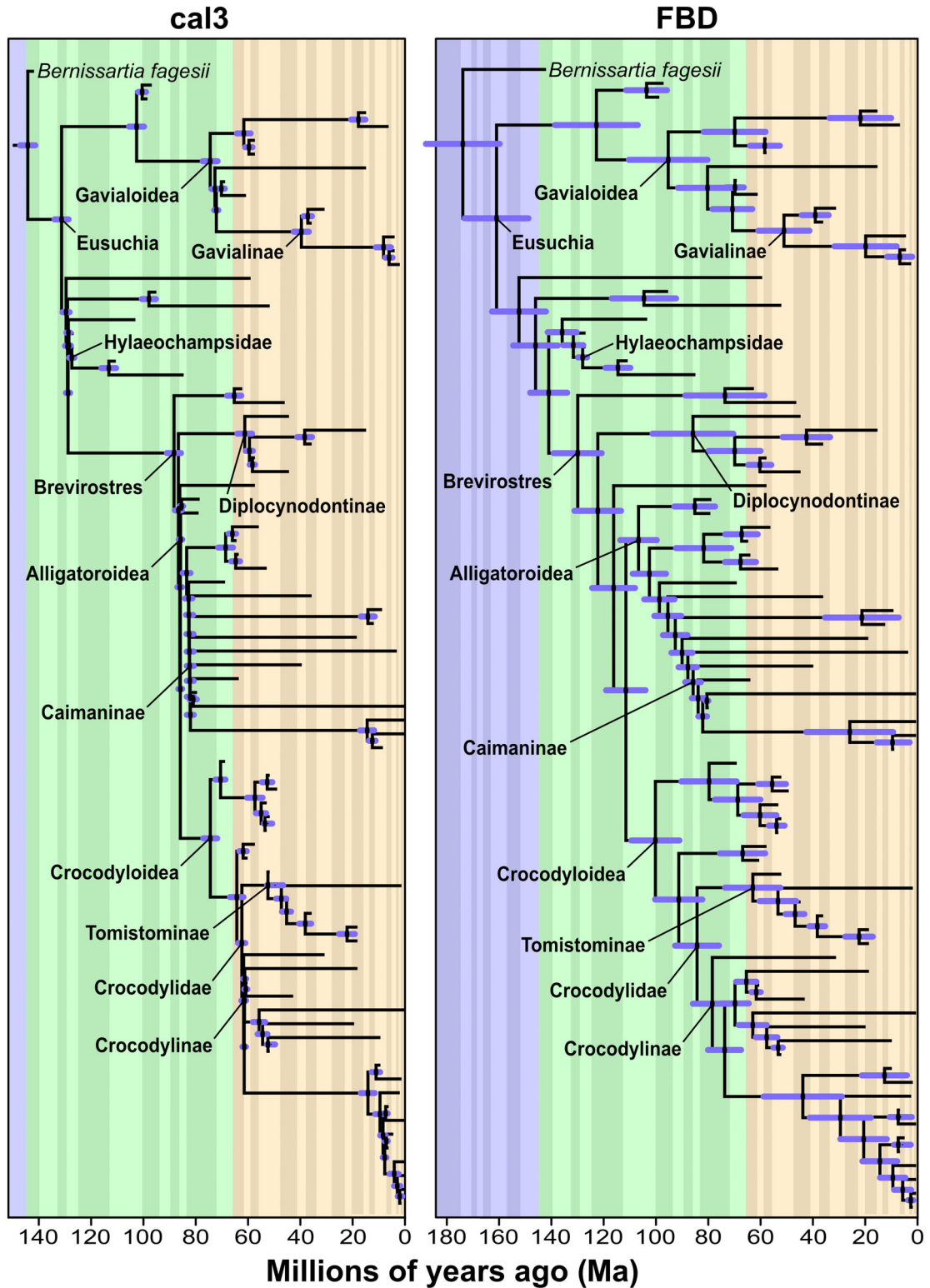
FIG. 5. Phylogenetic tree of Brevirostres, based on our modified version of Groh *et al.* (2020) with the four rogue taxa removed. Origination times were estimated with FBD and cal3.

2010; Brochu *et al.* 2012; Godoy *et al.* 2019), whereas others propose a post K/Pg boundary origin (Salisbury *et al.* 2006; Oaks 2011; Puértolas *et al.* 2011). Results from the G21 topology mirror this divide (Fig. 5): cal3 supports a diversification burst in Crocodylidae shortly after the K/Pg boundary, with Tomistominae, as well as Crocodylinae and multiple less diverse crocodyline groups diverging in quick succession. FBD, by contrast, favours a more gradual diversification (Fig. 5), taking place mostly during the Late Cretaceous after the origin of Crocodylidae during the middle Cretaceous (Table 4) and potentially fuelled by the hotter climatic conditions of the middle to Late Cretaceous (Mannion *et al.* 2015; O'Brien *et al.* 2017; Solórzano *et al.* 2019). The history supported by the mean node age estimates for the SB21 topology is similar, although the estimates for Crocodylidae are younger than those provided by the G21 topology. The SB21 trees support a Maastrichtian (FBD) or early Eocene (cal3) origin for Crocodylidae and Mekosuchinae (Fig. 3). Both scenarios can be linked to potential causal abiotic factors (see below), making it difficult to prefer one over the other.

Crocodylinae has previously been estimated to have originated during the middle–late Palaeogene or early Neogene, by both morphological (Salisbury *et al.* 2006; Puértolas *et al.* 2011; Lee & Yates 2018) and molecular (Roos *et al.* 2007; Oaks 2011) studies (Table 1). Our mean node age estimates for the SB21 topology mirror these dates, with 24 Ma (cal3) and 44 Ma (FBD) found for Crocodylinae. Our origination time estimates for the G21 topology are substantially older, with 61 Ma (cal3) and 79 Ma (FBD). This disagreement is mainly because of topological differences, namely: (1) the placement of the Paleocene family Planocraniidae as the closest sister group to Crocodylidae in G21; and (2) the definition of Crocodylinae and whether it should include the early Oligocene (33.9–28.1 Ma) *Crocodylus megarhinus*. According to Brochu (2000), *C. megarhinus* is an early-branching crocodyline, but it is not included in the SB21 topology, leading to the younger ages supported by the latter. The clade definitions used here (Groh *et al.* 2022, phylogenetics) are similar to those in Brochu (2003) and Gatesy *et al.* (2004): Crocodylinae encompasses all taxa that do not belong to Mekosuchinae (which is not included in the G21 dataset) and that are more closely related to extant taxa such as *C. niloticus* than to Tomistominae. Since *C. megarhinus* is included in the G21 dataset, this leads to older age estimates than for the SB21 topology. Thus, we regard the G21 node age estimates to be more reliable in this instance, and therefore support a diversification burst of early crocodyline species during the Paleocene, shortly after the K/Pg mass extinction, with most modern *Crocodylus* species and their closest relatives emerging during the Miocene.

The two different scenarios for the timing of crocodylid evolution suggested by cal3 and FBD apply also to Tomistominae in the G21 topology (this clade is represented only by two recent taxa in the SB21 topology). Previous morphological estimates have placed its origin in the Paleocene (Salisbury *et al.* 2006; Puértolas *et al.* 2011; Godoy *et al.* 2019). Unlike the latter trees, the G21 phylogenies were not constrained by molecular hypotheses, thus our estimates for the origin of *Tomistoma* are older than those in molecular trees (e.g. 16–30 Ma; Oaks 2011). All four of our time-scaling methods placed the most recent common ancestor of tomistomines in the early Palaeogene, from 49 Ma (cal3) to 62 Ma (FBD). However, the timing of the divergence of Tomistominae from the crocodyline lineage is dated differently, either during the Late Cretaceous (FBD), or the Paleocene (cal3), tied to the early Palaeogene diversification burst in Eusuchia (Fig. 5).

The third of the major eusuchian clades to originate during the Late Cretaceous was Alligatoroidea (Salisbury *et al.* 2006; Puértolas *et al.* 2011; Lee & Yates 2018; Table 1). After the removal of *Susisuchus jaguaribensis* from the G21 topology, the mean node age estimates from both the latter and the SB21 topologies suggest an origination of alligatoroids either between 95 and 106 Ma (FBD) or later at around 84–86 Ma (cal3), close to the age of the oldest known alligatoroid, *Albertochampsa langstoni* (Erickson 1972).

Diplocynodontinae, usually regarded as an alligatoroid clade (Brochu 1999; Delfino & Smith 2012), is placed as the sister clade to Crocodyloidea+Alligatoroidea in the G21 phylogenies, although it is still included in Brevirostres as defined herein. The earliest known putative diplocynodontine specimen, *Diplocynodon* sp., is from the Late Cretaceous (83.8–72.1 Ma) (Grandstaff *et al.* 1992). However, Grandstaff *et al.* (1992) did not provide any descriptions of the fossils, nor is the specimen described elsewhere in the literature, making its status as the only known Cretaceous diplocynodontine doubtful. The oldest confirmed diplocynodontine material is of early Eocene, and potentially late Paleocene, age (Martin *et al.* 2014*a*; Rio *et al.* 2020). The lineage leading to Diplocynodontinae diverged from the brevirostrine lineage during the Early to middle Cretaceous. The origination date for Diplocynodontinae itself is estimated at either Late Cretaceous (86 Ma, FBD) or Paleocene (61 Ma, cal3) in the G21 dataset. The mean node age estimates from the SB21 phylogeny are substantially younger than the G21 FBD estimate, both being Palaeogene in age (49 Ma (cal3) and 62 Ma (FBD)) (Fig. 4). These SB21 node ages are here regarded as unlikely because of the age of the earliest confirmed fossil material of this lineage. Thus, we support a Palaeogene origin for Diplocynodontinae.

Origination times for Globidonta differ strongly between molecular and morphological studies, with estimates around the K/Pg boundary derived from the former (Roos *et al.* 2007; Oaks 2011), and Late Cretaceous provided by the latter (Salisbury *et al.* 2006; Puértolas *et al.* 2011; Lee & Yates 2018; Mateus *et al.* 2018; Godoy *et al.* 2019) (Table 1). The oldest confirmed globidontan taxa are from the Late Cretaceous, *Stangerochampsa mccabei* (72.1–66.0 Ma; Wu *et al.* 1996) and *Albertochampsa langstoni* (83.6–72.1 Ma; Erickson 1972). There are potential remains of *Brachychampsa* sp. that are apparently the same age (83.8–72.1 Ma) (Storer 1993; Nessov 1995), but this cannot be verified from the available descriptions. Our cal3 dates (82 Ma and 83 Ma in SB21 and G21, respectively) are very similar to those obtained by morphological studies and the age of the earliest globidontans, whereas FBD mean node age estimates are slightly older (87 Ma and 102 Ma). As seen with the ages obtained for the other eusuchian lineages, cal3 suggests a Late Cretaceous diversification burst similar to that of Notosuchia (Solórzano *et al.* 2019), whereas FBD supports a more gradual scenario of alligatoroid evolution (Fig. 5) for both sets of topologies. Thus, despite the 20 myr age range provided by morphology, it seems that molecular age estimates for globidontan origin are too young.

By contrast to the G21 trees, the SB21 topologies contain both Alligatoridae and Alligatorinae. Mean node age estimates from our preferred methods corroborate their suggested presence before the K/Pg boundary (Brochu *et al.* 2012), with estimated clade ages of 68–83 Ma for Alligatoridae and 66–74 Ma for Alligatorinae with cal3, respectively. This overlaps with node age estimates within Globidonta in the G21 topologies, making a Late Cretaceous origin of Alligatoridae and early Palaeogene one for Alligatorinae likely.

Previous molecular and morphological studies have both placed the origin of Caimaninae after the K/Pg boundary (Salisbury *et al.* 2006; Roos *et al.* 2007; Oaks 2011; Puértolas *et al.* 2011; Lee & Yates 2018), anywhere between 20 and 58 Ma (Table 1). The oldest caimanine taxa are represented by *Eocaiman palaeocenicus* from the late Paleocene (Bona 2007) and a number of other remains from the early Paleocene (Brochu 2012; Pinheiro *et al.* 2013; Bona *et al.* 2018). By contrast, our estimates from both topologies are mostly in the Late Cretaceous, 82 Ma (cal3, G21 topology) to 78 Ma (FBD, SB21 topology) and 85 Ma (FBD, G21 topology), because of the altered topology and inclusion of several old caimanine species. Only the cal3 estimates for the SB21 topology are marginally younger than the K/Pg boundary, 66 Ma (Table 3), making a Late Cretaceous origin and subsequent early Palaeogene diversification for the clade probable.

Biotic and abiotic factors influencing neosuchian evolutionary history

The end-Triassic mass extinction included the loss of tetrapod groups such as Phytosauria and Rauisuchia that had at least some ecological similarities to crocodylomorphs (Toljagić & Butler 2013; Bronzati *et al.* 2015; Godoy *et al.* 2019). The proposed Early Jurassic origin of Neosuchia, and its diversification into Goniopholididae, Paralligatoridae, Atoposauridae, and the lineage leading to Eusuchia, might therefore represent an opportunistic replacement with the clade filling niches left vacant by the mass extinction. This radiation can be detected in both increased diversification rates and disparity among Early Jurassic crocodylomorphs (Toljagić & Butler 2013; Bronzati *et al.* 2015; Godoy *et al.* 2019). The end of the Early Jurassic marked the onset of warmer climates (Sellwood & Valdes 2008), with increases in sea surface temperature and sea level, both of which have been linked to the diversification of marine and non-marine crocodylomorphs (Martin *et al.* 2014*b*; Tennant *et al.* 2016*a*). This supports the scenario of a Middle to Late Jurassic origin of Tethysuchia and the diversification of a range of younger goniopholidid species.

During the Early Cretaceous, numerous environmental perturbations caused several tetrapod lineages with niches similar to those of early eusuchians to go extinct, such as some non-marine turtles, mammals and non-marine crocodylomorphs (Tennant *et al.* 2016*a*). This was followed by a short period of elevated sea level and temperatures (Carvalho *et al.* 2010; Tennant *et al.* 2016*a*, *b*). The extinction of the above-mentioned lineages, coupled with these abiotic factors, could have led to an increase in the number of the ecological niches available for early eusuchians during the Early Cretaceous. Increased temperatures are linked to higher evolutionary and diversification rates in Crocodylomorpha (Markwick 1998; Tennant *et al.* 2016*b*; Solórzano *et al.* 2019; Stubbs *et al.* 2021), potentially facilitating eusuchian diversification and supporting an Early Cretaceous origin of Eusuchia. Moreover, hotter climates during the early Late Cretaceous (Brochu 2003; Carvalho *et al.* 2010; Stubbs *et al.* 2021), including the Cretaceous Thermal Maximum with high global sea surface temperatures (O'Brien *et al.* 2017; Solórzano *et al.* 2019), probably promoted the evolution of the three major eusuchian lineages: Crocodyloidea, Gavialoidea and Alligatoroidea.

The K/Pg mass extinction witnessed severe reductions in the diversity of many tetrapod lineages, including the loss of all non-avian dinosaurs. This increased availability of niches and resources led to diversification bursts in several vertebrate clades, such as neornithine birds and placental mammals (de Celis *et al.* 2019). The early Palaeogene was also characterized by the

Paleocene–Eocene Thermal Maximum (PETM) (Röhl *et al.* 2007) and the Early Eocene Climatic Optimum (EECO) (Lauretano *et al.* 2015). This combination of opportunistic replacements immediately after the K/Pg extinction, and higher temperatures during the Paleocene–Eocene, potentially led to increased speciation rates among eusuchians. These conditions promoted the evolution of Gavialinae, Tomistominae, Diplocynodontinae, Caimaninae, Mekosuchinae and early Crocodylinae. In addition, the diversification of Caimaninae was potentially linked to range expansion facilitated by an ephemeral North–South America connection that was present during the Late Cretaceous (Hastings *et al.* 2013; Poropat *et al.* 2016) and was part of a wider increase in alligatoroid diversity during the Paleocene (Bronzati *et al.* 2015; de Celis *et al.* 2019).

Finally, the relatively warm periods of the Miocene led to the evolution of most modern *Crocodylus* species and their closest relatives (de Celis *et al.* 2019). Multiple dispersal events took place subsequently, fuelled by several advantageous life history traits within *Crocodylus*, such as habitat generalism and saltwater tolerance (Nicolaï & Matzke 2019), with increases in diversity during warmer periods. However, the general global cooling trend observed over the past 30 myr resulted in a decline in the geographic ranges of crocodiles, leading to the greatly reduced diversity present today (Markwick 1998; Mannion *et al.* 2015).

CONCLUSION

We have used an updated phylogeny (based on Groh *et al.* 2020) and a supertree (Stockdale & Benton 2021) to examine the origination dates of major neosuchian clades and evaluate the behaviour of newer stochastic time-scaling methods (cal3 and extended Hedman (EH)) in the presence of different types of data compared to fossilized birth–death (FBD) and smoothed ghost lineage analysis (sGLA). All four time-scaling methods across both sets of topologies agreed that the lineages leading to the main neosuchian clades (Tethysuchia, Goniopholididae, Atoposauridae, Paralligatoridae, Eusuchia) had diverged by the Early Jurassic. Similarly, the three main crocodylian superfamilies (Gavialoidea, Crocodyloidea, Alligatoroidea) appeared before the K/Pg boundary, possibly in response to the high temperatures of the Cretaceous Thermal Maximum, which occurred in the Turonian. Two different scenarios of eusuchian evolution are supported in both sets of topologies: a rapid diversification burst of Eusuchia, and in particular, Crocodylidae, after the K/Pg boundary, or a more gradual evolution of the different crocodylid lineages (including Tomistominae) beginning during the Late Cretaceous. Our results also

support the inferred presence of Caimaninae before the K/Pg boundary, contrary to recent molecular dating estimates.

In general, stochastic time-scaling methods are not more reliable than others: cal3 is the most robust method with regards to its relative insensitivity to solitary taxon exclusions and minor changes in topology; however, EH is affected by these issues to a similar degree as sGLA and FBD. For the majority of nodes, EH provides the oldest age estimates (together with larger standard deviations), whereas cal3 provides the youngest ages and narrowest standard deviations, in part because it also allows zero-length branches. In addition, EH and sGLA are particularly influenced by sampling biases and taxon coverage in the dated topologies. Inclusion of the oldest-known taxon of each major taxonomic group in the tree is paramount in order to obtain more realistic estimates for all four methods, more so than full taxon coverage. As such, the use of supertrees instead of MPTs cannot be recommended without caveats, because supertrees rely on their source trees containing the oldest-known taxon of each clade. If both MPTs and supertrees contain the oldest-known taxa, the increased number of taxon sampling in supertrees does not per se provide better age estimates, unless sampling covers groups not represented in the MPTs. In addition, supertrees can potentially suffer from a number of other problems, such as non-independence of source trees, novel relationships not represented in any of the input MPTs, and longer resulting trees than those based on supermatrices (Gatesy *et al.* 2004; Bennett *et al.* 2008; Haeseler 2012; Janies *et al.* 2013). Larger datasets can provide similar amounts of taxon coverage to supertrees and should not be discounted (Laing *et al.* 2018).

Based on our results, we recommend the combined use of cal3 and FBD as preferred origination time estimation methods. Given the artefactual bimodal age estimate distributions of sGLA and the relatively arbitrary, linear criteria of scaling branch lengths, we suggest that this approach should be avoided (see also Bapst 2013). Application of EH should be treated with caution, given the extremely old ages that it tends to produce, and the greater sensitivity of these ages to variation in phylogenetic topology. Nevertheless, EH is potentially a better choice when working with datasets with near-complete taxon sampling and high proportions of singleton taxa, in order to avoid the problems caused by the latter when applying cal3. Generally, the application of a single method to date just one tree cannot be recommended, because this would only sample a (not necessarily accurate) subset of possible ages. Future studies that require dated morphological trees need to do more to justify their choice of dating method(s), should build trees with the needs of dating in mind (e.g. sampling of the oldest putative clade members), and should tailor their choice of

method to the properties of the available trees and the nature of the target group's fossil record.

Several potentially fruitful lines of enquiry into the accuracy of origination time estimation methods can be identified. First, our conclusions are based on the application of multiple methods to only two independent datasets (and should be regarded as a case study): this raises the question of whether the phenomena noted above are unique to neosuchians, or if they are repeated across many different clades? Second, we should investigate whether clade age estimates for given nodes are converging on a consensus through historical research time. New fossil discoveries are likely to produce a general trend towards finding older origination times, but there is likely to come a point where the 'correct' answer is approached. It would be useful to pinpoint where we are currently with respect to this scenario of initially wide uncertainty/high error followed by gradually increasing consensus, and how this trend varies between different clades. Finally, our recommendations for method selection are necessarily somewhat qualitative at this stage: it would be helpful to identify, for example, the proportion of singleton taxa and/or the extent of taxon coverage that determines whether Calc3 or EH yields the more accurate origination time estimates, through both simulations and more empirical case studies.

DATA ARCHIVING STATEMENT

Data for this study are available in the Dryad Digital Repository: https://doi.org/10.5061/dryad.4f4qrfj89. Data are divided into two different datasets:
Phylogenetics: Contains character lists, character scores, tree files, consensus trees, clade definitions, a list of synapomorphies for each clade, and a list of changes compared to Groh *et al.* (2020).
Timescaling: Contains the R code used for analysis, raw times and data files, estimated ages for all clades and trees by each method and time-scaled trees for each method.

Editor. Roger Benson

REFERENCES

ADAMS, T. L. 2014. Small crocodyliform from the Lower Cretaceous (late Aptian) of central Texas and its systematic relationship to the evolution of Eusuchia. *Journal of Paleontology*, **88**, 1031–1049.

ALLEN, B. J., STUBBS, T. L., BENTON, M. J. and PUTTICK, M. N. 2019. Archosauromorph extinction selectivity during the Triassic–Jurassic mass extinction. *Palaeontology*, **62**, 211–224.

ANDRES, B. 2012. The early evolutionary history and adaptive radiation of the Pterosauria. *Acta Geologica Sinica - English Edition*, **86**, 1356–1365.

BAPST, D. W. 2012. paleotree: an R package for paleontological and phylogenetic analyses of evolution. *Methods in Ecology & Evolution*, **3**, 803–807.

BAPST, D. W. 2013. A stochastic rate-calibrated method for time-scaling phylogenies of fossil taxa. *Methods in Ecology & Evolution*, **4**, 724–733.

BAPST, D. W. 2014. Assessing the effect of time-scaling methods on phylogeny-based analyses in the fossil record. *Paleobiology*, **40**, 331–351.

BAPST, D. W. and HOPKINS, M. J. 2017. Comparing cal3 and other a posteriori time-scaling approaches in a case study with the pterocephaliid trilobites. *Paleobiology*, **43**, 49–67.

BAPST, D. W., WRIGHT, A. M., MATZKE, N. J. and LLOYD, G. T. 2016. Topology, divergence dates, and macroevolutionary inferences vary between different tip-dating approaches applied to fossil theropods (Dinosauria). *Biology Letters*, **12**, 20160237.

BELL, M. A. and LLOYD, G. T. 2014. strap: an R package for plotting phylogenies against stratigraphy and assessing their stratigraphic congruence. *Palaeontology*, **58**, 1–11.

BENNETT, G., LAPOINT, R. and O'GRADY, P. 2008. The potential and peril of the supertree approach: a response to van der Linde and Houle. *Insect Systematics & Evolution*, **39**, 269–280.

BENSON, R. B., HUNT, G., CARRANO, M. T. and CAMPIONE, N. 2018. Cope's rule and the adaptive landscape of dinosaur body size evolution. *Palaeontology*, **61**, 13–48.

BONA, P. 2007. Una nueva especie de Eocaiman Simpson (Crocodylia, Alligatoridae) del Paleoceno Inferior de Patagonia. *Ameghiniana*, **44**, 435–445.

BONA, P., EZCURRA, M. D., BARRIOS, F., and FERNANDEZ, B. M. V. 2018. A new Palaeocene crocodylian from southern Argentina sheds light on the early history of caimanines. *Proceedings of the Royal Society B*, **285**, 20180843.

BOUCKAERT, R., HELED, J., KÜHNERT, D., VAUGHAN, T., WU, C.-H., XIE, D., SUCHARD, M. A., RAMBAUT, A. and DRUMMOND, A. J. 2014. BEAST 2: a software platform for Bayesian evolutionary analysis. *PLoS Computational Biology*, **10**, e1003537.

BRAZEAU, M. D. 2011. Problematic character coding methods in morphology and their effects. *Biological Journal of the Linnean Society*, **104**, 489–498.

BROCHU, C. A. 1997. A review of "Leidyosuchus" (Crocodyliformes, Eusuchia) from the Cretaceous through Eocene of North America. *Journal of Vertebrate Paleontology*, **17**, 679–697.

BROCHU, C. A. 1999. Phylogenetics, taxonomy, and historical biogeography of Alligatoroidea. *Journal of Vertebrate Paleontology*, **19**, 9–100.

BROCHU, C. A. 2000. Phylogenetic relationships and divergence timing of *Crocodylus* based on morphology and the fossil record. *Copeia*, **2000**, 657–673.

BROCHU, C. A. 2003. Phylogenetic approaches toward Crocodylian history. *Annual Review of Earth & Planetary Sciences*, **31**, 357–397.

BROCHU, C. A. 2004. Alligatorine phylogeny and the status of *Allognathosuchus* Mook, 1921. *Journal of Vertebrate Paleontology*, **24**, 857–873.

BROCHU, C. A. 2012. Phylogenetic relationships of Palaeogene ziphodont eusuchians and the status of *Pristichampsus* Gervais, 1853. *Earth & Environmental Science Transactions of the Royal Society of Edinburgh*, **103**, 521–550.

BROCHU, C. A., PARRIS, D. C., GRANDSTAFF, B. S., DENTON, R. K. Jr and GALLAGHER, W. B. 2012. A new species of *Borealosuchus* (Crocodyliformes, Eusuchia) from the Late Cretaceous–early Paleogene of New Jersey. *Journal of Vertebrate Paleontology*, **32**, 105–116.

BRONZATI, M., MONTEFELTRO, F. C. and LANGER, M. C. 2012. A species-level supertree of Crocodyliformes. *Historical Biology*, **24**, 598–606.

BRONZATI, M., MONTEFELTRO, F. C. and LANGER, M. C. 2015. Diversification events and the effects of mass extinctions on Crocodyliformes evolutionary history. *Open Science*, **2**, 140385.

BRUSATTE, S. L. 2011. Calculating the tempo of morphological evolution: rates of discrete character change in a phylogenetic context. 53–74. *In* ELEWA, M. T. (ed.) *Computational paleontology*. Springer.

BRUSATTE, S. L., BENTON, M. J., RUTA, M. and LLOYD, G. T. 2008. Superiority, competition, and opportunism in the evolutionary radiation of dinosaurs. *Science*, **321**, 1485–1488.

BUSCALIONI, A. D. and SANZ, L 1988. Phylogenetic relationships of the Atoposauridae (Archosauria, Crocodylomorpha). *Historical Biology*, **1**, 233–250.

CARVALHO, I. DE S., GASPARINI, Z. B. DE, SALGADO, L. and VASCONCELLOS, F. M. DE and MARINHO, T. DA S. 2010. Climate's role in the distribution of the Cretaceous terrestrial Crocodyliformes throughout Gondwana. *Palaeogeography, Palaeoclimatology, Palaeoecology*, **297**, 252–262.

CLARK, J. M. and NORELL, M. A. 1992. The Early Cretaceous crocodylomorph *Hylaeochampsa vectiana* from the Wealden of the Isle of Wight. *American Museum Novitates*, **3032**, 1–19.

COHEN, K. M., FINNEY, S. C., GIBBARD, P. L. and FAN, J.-X. 2013. The ICS international chronostratigraphic chart. *Episodes*, **36**, 199–204.

ANDRADE, M. B. DE, EDMONDS, R., BENTON, M. J. and SCHOUTEN, R. 2011. A new Berriasian species of *Goniopholis* (Mesoeucrocodylia, Neosuchia) from England, and a review of the genus. *Zoological Journal of the Linnean Society*, **163**, S66–S108.

DE CELIS, A., NARVÁEZ, I. and ORTEGA, F. 2019. Spatiotemporal palaeodiversity patterns of modern crocodiles (Crocodyliformes: Eusuchia). *Zoological Journal of the Linnean Society*, **2**, 635–656.

DELFINO, M. and SMITH, T. 2012. Reappraisal of the morphology and phylogenetic relationships of the middle Eocene alligatoroid *Diplocynodon deponiae* (Frey, Laemmert, and Riess, 1987) based on a three-dimensional specimen. *Journal of Vertebrate Paleontology*, **32**, 1358–1369.

DELFINO, M., CODREA, V., FOLIE, A., DICA, P., GODEFROIT, P. and SMITH, T. 2008. A complete skull of *Allodaposuchus precedens* Nopcsa, 1928 (Eusuchia) and a reassessment of the morphology of the taxon based on the Romanian remains. *Journal of Vertebrate Paleontology*, **28**, 111–122.

DOS REIS, M., DONOGHUE, P. C. J. and YANG, Z. 2014. Neither phylogenomic nor palaeontological data support a Palaeogene origin of placental mammals. *Biology Letters*, **10**, 20131003.

ERICKSON, B. R. 1972. *Albertochampsa langstoni*, gen. et. sp. nov., a new alligator from the Cretaceous of Alberta. *Scientific Publications of the Science Museum of Minnesota (NS)*, **2**, 1–13.

FIORELLI, L. E. and CALVO, J. 2008. New remains of Notosuchus terrestris Woodward, 1896 (Crocodyliformes: Mesoeucrocodylia) from Late Cretaceous of Neuquén, Patagonia, Argentina. *Arquivos do Museum Nacional, Rio de Janeiro*, **66**, 83–124.

FOOTE, M. 1997. Estimating taxonomic durations and preservation probability. *Paleobiology*, 278–300.

FORTIER, D. C. and SCHULTZ, C. L. 2009. A New neosuchian crocodylomorph (Crocodyliformes, Mesoeucrocodylia) from the Early Cretaceous of North-East Brazil. *Palaeontology*, **52**, 991–1007.

FORTIER, D., PEREA, D. and SCHULTZ, C. 2011. Redescription and phylogenetic relationships of *Meridiosaurus vallisparadisi*, a pholidosaurid from the Late Jurassic of Uruguay. *Zoological Journal of the Linnean Society*, **163**, S257–S272.

GATESY, J., BAKER, R. H. and HAYASHI, C. 2004. Inconsistencies in arguments for the supertree approach: supermatrices versus supertrees of Crocodylia. *Systematic Biology*, **53**, 342–355.

GAVRYUSHKINA, A., WELCH, D., STADLER, T. and DRUMMOND, A. J. 2014. Bayesian inference of sampled ancestor trees for epidemiology and fossil calibration. *PLoS Computational Biology*, **10**, e1003919.

GODOY, P. L., BENSON, R. B. J., BRONZATI, M. and BUTLER, R. J. 2019. The multi-peak adaptive landscape of crocodylomorph body size evolution. *BMC Evolutionary Biology*, **19**, 167.

GOLOBOFF, P. A. 2014. Extended implied weighting. *Cladistics*, **30**, 260–272.

GOLOBOFF, P. A. and CATALANO, S. A. 2016. TNT version 1.5, including a full implementation of phylogenetic morphometrics. *Cladistics*, **32**, 221–238.

GRANDSTAFF, B. S., PARRIS, D. C., DENTON, R. K. Jr and GALLAGHER, W. B. 1992. *Alphadon* (Marsupialia) and Multituberculata (Allotheria) in the Cretaceous of eastern North America. *Journal of Vertebrate Paleontology*, **12**, 217–222.

GRIGG, G., KIRSHNER, D. and SHINE, R. 2015. *Biology and evolution of crocodylians*. Cornell University Press.

GROH, S. S., UPCHURCH, P., BARRETT, P. M. and DAY, J. J. 2020. The phylogenetic relationships of neosuchian crocodiles and their implications for the convergent evolution of the longirostrine condition. *Zoological Journal of the Linnean Society*, **188**, 473–506.

GROH, S. S., UPCHURCH, P., BARRETT, P. M. and DAY, J. J. 2022. How to date a crocodile – estimation of neosuchian clade ages and a comparison of the performance of four time-scaling methods. *Dryad Digital Repository*. https://doi.org/10.5061/dryad.4f4qrfj89

HAESELER, A. VON 2012. Do we still need supertrees? *BMC Biology*, **10**, 13.

HART, L. J. 2020. Taxonomic clarifications concerning the crocodyliform genus *Isisfordia*. *PeerJ*, **8**, e8630.

HART, L. J., BELL, P. R., SMITH, E. T. and SALISBURY, S. W. 2019. *Isisfordia molnari* sp. nov., a new basal eusuchian from the mid-Cretaceous of Lightning Ridge, Australia. *PeerJ*, **7**, e7166.

HASTINGS, A. K., BLOCH, J. I., CADENA, E. A. and JARAMILLO, C. A. 2010. A new small short-snouted dyrosaurid (Crocodylomorpha, Mesoeucrocodylia) from the Paleocene of Northeastern Colombia. *Journal of Vertebrate Paleontology*, **30**, 139–162.

HASTINGS, A. K., BLOCH, J. I., JARAMILLO, C. A., RINCON, A. F. and MACFADDEN, B. J. 2013. Systematics and biogeography of crocodylians from the Miocene of Panama. *Journal of Vertebrate Paleontology*, **33**, 239–263.

HASTINGS, A. K., BLOCH, J. I. and JARAMILLO, C. A. 2014. A new blunt-snouted dyrosaurid, *Anthracosuchus balrogus* gen. et sp. nov. (Crocodylomorpha, Mesoeucrocodylia), from the Palaeocene of Colombia. *Historical Biology*, 1–23.

HEATH, T. A., HUELSENBECK, J. P. and STADLER, T. 2014. The fossilized birth–death process for coherent calibration of divergence-time estimates. *Proceedings of the National Academy of Sciences*, **111**, E2957–E2966.

HEDMAN, M. M. 2010. Constraints on clade ages from fossil outgroups. *Paleobiology*, **36**, 16–31.

HOLLIDAY, C. M. and GARDNER, N. M. 2012. A new eusuchian crocodyliform with novel cranial Integument and Its significance for the origin and evolution of Crocodylia. *PLoS One*, **7**, e3047.

HUNT, G. and CARRANO, M. T. 2010. Models and methods for analyzing phenotypic evolution in lineages and clades. *The Paleontological Society Papers*, **16**, 245–269.

JANIES, D. A., STUDER, J., HANDELMAN, S. K. and LINCHANGCO, G. 2013. A comparison of supermatrix and supertree methods for multilocus phylogenetics using organismal datasets. *Cladistics*, **29**, 560–566.

JOUVE, S., IAROCHENE, M., BOUYA, B. and AMAGHZAZ, M. 2005. A new dyrosaurid crocodyliform from the Palaeocene of Morocco and a phylogenetic analysis of Dyrosauridae. *Acta Palaeontologica Polonica*, **50**, 581–594.

JOUVE, S., BOUYA, B., AMAGHZAZ, M. and MESLOUH, S. 2015. *Maroccosuchus zennaroi* (Crocodylia: Tomistominae) from the Eocene of Morocco: phylogenetic and palaeobiogeographical implications of the basalmost tomistomine. *Journal of Systematic Palaeontology*, **13**, 421–445.

LAING, A. M., DOYLE, S., GOLD, M. E. L., NESBITT, S. J., O'LEARY, M. A., TURNER, A. H., WILBERG, E. W. and POOLE, K. E. 2018. Giant taxon-character matrices: the future of morphological systematics. *Cladistics*, **34**, 333–335.

LAURETANO, V., LITTLER, K., POLLING, M., ZACHOS, J. C. and LOURENS, L. J. 2015. Frequency, magnitude and character of hyperthermal events at the onset of the Early Eocene Climatic Optimum. *Climate of the Past*, **11**, 1313–1324.

LAURIN, M., CANOVILLE, A. and QUILHAC, A. 2009. Use of paleontological and molecular data in supertrees for comparative studies: the example of lissamphibian femoral microanatomy. *Journal of Anatomy*, **215**, 110–123.

LEE, M. S. Y. and YATES, A. M. 2018. Tip-dating and homoplasy: reconciling the shallow molecular divergences of modern gharials with their long fossil record. *Proceedings of the Royal Society B*, **285**, 20181071.

LLOYD, G. T., WANG, S. C. and BRUSATTE, S. L. 2012. Identifying heterogeneity in rates of morphological evolution: discrete character change in the evolution of lungfish (Sarcopterygii; Dipnoi). *Evolution*, **66**, 330–348.

LLOYD, G. T., BAPST, D. W., FRIEDMAN, M. and DAVIS, K. E. 2016. Probabilistic divergence time estimation without branch lengths: dating the origins of dinosaurs, avian flight and crown birds. *Biology Letters*, **12**, 20160609.

MANNION, P. D., BENSON, R. B. J., CARRANO, M. T., TENNANT, J. P., JUDD, J. and BUTLER, R. J. 2015. Climate constrains the evolutionary history and biodiversity of crocodylians. *Nature Communications*, **6**, 8438.

MANNION, P. D., CHIARENZA, A. A., GODOY, P. L. and CHEAH, Y. N. 2019. Spatiotemporal sampling patterns in the 230 million year fossil record of terrestrial crocodylomorphs and their impact on diversity. *Palaeontology*, **62**, 615–637.

MARKWICK, P. J. 1998. Fossil crocodilians as indicators of Late Cretaceous and Cenozoic climates: implications for using palaeontological data in reconstructing palaeoclimate. *Palaeogeography, Palaeoclimatology, Palaeoecology*, **137**, 205–271.

MARTIN, J. E. and DELFINO, M. 2010. Recent advances in the comprehension of the biogeography of Cretaceous European eusuchians. *Palaeogeography, Palaeoclimatology, Palaeoecology*, **293**, 406–418.

MARTIN, J. E. and LAUPRASERT, K. 2010. A new primitive alligatorine from the Eocene of Thailand: relevance of Asiatic members to the radiation of the group. *Zoological Journal of the Linnean Society*, **158**, 608–628.

MARTIN, J. E., RABI, M. and CSIKI, Z. 2010. Survival of *Theriosuchus* (Mesoeucrocodylia: Atoposauridae) in a Late Cretaceous archipelago: a new species from the Maastrichtian of Romania. *Naturwissenschaften*, **97**, 845–854.

MARTIN, J. E., SMITH, T., DE LAPPARENT DE BROIN, F., ESCUILLIÉ, F. and DELFINO, M. 2014*a*. Late Palaeocene eusuchian remains from Mont de Berru, France, and the origin of the alligatoroid *Diplocynodon*. *Zoological Journal of the Linnean Society*, **172**, 867–891.

MARTIN, J. E., AMIOT, R., LÉCUYER, C. and BENTON, M. J. 2014*b*. Sea surface temperature contributes to

marine crocodylomorph evolution. *Nature Communications*, **5**, 1–7.

MARTIN, J. E., RASLAN-LOUBATIÉ, J. and MAZIN, J.-M. 2016. Cranial anatomy of *Pholidosaurus purbeckensis* from the Lower Cretaceous of France and its bearing on pholidosaurid affinities. *Cretaceous Research*, **66**, 43–59.

MARTINELLI, A. G. 2003. New cranial remains of the bizarre notosuchid *Comahuesuchus brachybuccalis* (Archosauria, Crocodyliformes) from the Late Cretaceous of Rio Negro Province (Argentina). *Ameghiniana*, **40**, 559–572.

MASSONNE, T., VASILYAN, D., RABI, M. and BÖHME, M. 2019. A new alligatoroid from the Eocene of Vietnam highlights an extinct Asian clade independent from extant *Alligator sinensis*. *PeerJ*, **7**, e7562.

MATEUS, O., PUÉRTOLAS-PASCUAL, E. and CALLAPEZ, P. M. 2018. A new eusuchian crocodylomorph from the Cenomanian (Late Cretaceous) of Portugal reveals novel implications on the origin of Crocodylia. *Zoological Journal of the Linnean Society*, **186**, 501–528.

MATZKE, N. J. and WRIGHT, A. 2016. Inferring node dates from tip dates in fossil Canidae: the importance of tree priors. *Biology letters*, **12**, 20160328.

MOLNAR, R. E. and WILLIS, P. M. A. 2001. New crocodyliform material from the Early Cretaceous Griman Creek Formation, at Lightning Ridge. New South Wales. 75–82. *In* GRIGG, G. C., SEEBACHER, F. and FRANKLIN, C. E. (eds). *Crocodilian biology and evolution*. Surrey Beatty & Sons.

MONTEFELTRO, F. C., LARSSON, H. C. E., FRANÇA, M. A. G. DE and LANGER, M. C. 2013. A new neosuchian with Asian affinities from the Jurassic of northeastern Brazil. *Naturwissenschaften*, **100**, 835–841.

NARVÁEZ, I., BROCHU, C. A., ESCASO, F., PÉREZ-GARCÍA, A. and ORTEGA, F. 2015. New crocodyliforms from southwestern Europe and definition of a diverse clade of European Late Cretaceous basal eusuchians. *PLoS One*, **10**, e014067.

NESBITT, S. J. 2011. The early evolution of archosaurs: relationships and the origin of major clades. *Bulletin of the American Museum of Natural History*, **352**, 1–292.

NESSOV, L. A. 1995. [*Dinosaurs of northern Eurasia: new data about assemblages, ecology and paleobiogeography*]. Institute for Scientific Research on the Earth's Crust, St. Petersburg State University, 156 pp.

NICOLAÏ, M. P. J. and MATZKE, N. J. 2019. Trait-based range expansion aided in the global radiation of Crocodylidae. *Global Ecology & Biogeography*, **28**, 1244–1258.

NORELL, M. A., NOVACEK, M. J. and WHEELER, Q. D. 1992. Taxic origin and temporal diversity: the effect of phylogeny. 89–118. *In* NOVACEK, M. J. and WHEELER, Q. D. (eds) *Extinction and phylogeny*. Columbia University Press.

NORELL, M., CLARK, J. M. and HUTCHISON, J. H. 1994. The Late Cretaceous alligatoroid *Brachychampsa montana* (Crocodylia): new material and putative relationships. *American Museum Novitates*, **3116**, 1–26.

OAKS, J. R. 2011. A time-calibrated species tree of Crocodylia reveals a recent radiation of the true crocodiles. *Evolution*, **65**, 3285–3297.

O'BRIEN, C. L., ROBINSON, S. A., PANCOST, R. D., SINNINGHE DAMSTÉ, J. S., SCHOUTEN, S., LUNT, D. J., ALSENZ, H., BORNEMANN, A., BOTTINI, C., BRASSELL, S. C., FARNSWORTH, A., FORSTER, A., HUBER, B. T., INGLIS, G. N., JENKYNS, H. C., LINNERT, C., LITTLER, K., MARKWICK, P., MCANENA, A., MUTTERLOSE, J., NAAFS, B. D. A., PÜTTMANN, W., SLUIJS, A., VAN HELMOND, N. A. G. M., VELLEKOOP, J., WAGNER, T. and WROBEL, N. E. 2017. Cretaceous sea-surface temperature evolution: constraints from TEX_{86} and planktonic foraminiferal oxygen isotopes. *Earth-Science Reviews*, **172**, 224–247.

O'LEARY, M. A., BLOCH, J. I., FLYNN, J. J., GAUDIN, T. J., GIALLOMBARDO, A., GIANNINI, N. P., GOLDBERG, S. L., KRAATZ, B. P., LUO, Z.-X., MENG, J., NI, X., NOVACEK, M. J., PERINI, F. A., RANDALL, Z. S., ROUGIER, G. W., SARGIS, E. J., SILCOX, M. T., SIMMONS, N. B., SPAULDING, M., VELAZCO, P. M., WEKSLER, M., WIBLE, J. R. and CIRRANELLO, A. L. 2013. The placental mammal ancestor and the post–K-Pg radiation of placentals. *Science*, **339**, 662–667.

PARADIS, E. and SCHLIEP, K. 2019. ape 5.0: an environment for modern phylogenetics and evolutionary analyses in R. *Bioinformatics*, **35**, 526–528.

PATIÑO, J. and VANDERPOORTEN, A. 2015. Macaronesia is a departure gate of anagenetic speciation in the moss genus *Rhynchostegiella*. *Journal of Biogeography*, **42**, 2122–2130.

PINHEIRO, A. E. P., FORTIER, D. C., POL, D., CAMPOS, D. A. and BERGQVIST, L. P. 2013. A new eocaiman (Alligatoridae, Crocodylia) from the Itaboraí Basin, Paleogene of Rio de Janeiro, Brazil. *Historical Biology*, **25**, 327–337.

PIRAS, P. 2007. Phylogenetic position of the crocodylian *Megadontosuchus arduini* and tomistomine palaeobiogeography. *Acta Palaeontologica Polonica*, **52**, 315.

POL, D. 2005. Postcranial remains of *Notosuchus terrestris* Woodward (Archosauria: Crocodyliformes) from the upper Cretaceous of Patagonia, Argentina. *Ameghiniana*, **42**, 21–38.

POL, D. and GASPARINI, Z. 2009. Skull anatomy of *Dakosaurus andiniensis* (Thalattosuchia: Crocodylomorpha) and the phylogenetic position of Thalattosuchia. *Journal of Systematic Palaeontology*, **7**, 163–197.

POL, D., TURNER, A. H. and NORELL, M. A. 2009. Morphology of the Late Cretaceous crocodylomorph *Shamosuchus djadochtaensis* and a discussion of neosuchian phylogeny as related to the origin of Eusuchia. *Bulletin of the American Museum of Natural History*, **324**, 1–103.

POROPAT, S. F., MANNION, P. D., UPCHURCH, P., HOCKNULL, S. A., KEAR, B. P., KUNDRÁT, M., TISCHLER, T. R., SLOAN, T., SINAPIUS, G. H. K., ELLIOTT, J. A. and ELLIOTT, D. A. 2016. New Australian sauropods shed light on Cretaceous dinosaur palaeobiogeography. *Scientific Reports*, **6**, 34467.

PUÉRTOLAS, E., CANUDO, J. I. and CRUZADO-CABALLERO, P. 2011. A new crocodylian from the Late Maastrichtian of Spain: implications for the initial radiation of crocodyloids. *PLoS One*, **6**, e20011.

PUÉRTOLAS-PASCUAL, E., CANUDO, J. I. and MORENO-AZANZA, M. 2014. The eusuchian

crocodylomorph *Allodaposuchus subjuniperus* sp. nov., a new species from the latest Cretaceous (upper Maastrichtian) of Spain. *Historical Biology*, 26, 91–109.

PÜSCHEL, H. P., O'REILLY, J. E., PISANI, D. and DONOGHUE, P. C. J. 2020. The impact of fossil stratigraphic ranges on tip-calibration, and the accuracy and precision of divergence time estimates. *Palaeontology*, 63, 67–83.

PUTTICK, M. N., KRIWET, J., WEN, W., HU, S., THOMAS, G. H. and BENTON, M. J. 2017. Body length of bony fishes was not a selective factor during the biggest mass extinction of all time. *Palaeontology*, 60, 727–741.

R CORE TEAM 2013. R: a language and environment for statistical computing. R Foundation for Statistical Computing, Vienna, Austria. https://www.R-project.org

RIO, J. P., MANNION, P. D., TSCHOPP, E., MARTIN, J. E. and DELFINO, M. 2020. Reappraisal of the morphology and phylogenetic relationships of the alligatoroid crocodylian *Diplocynodon hantoniensis* from the late Eocene of the United Kingdom. *Zoological Journal of the Linnean Society*, 188, 579–629.

ROGERS, J. V. 2003. *Pachycheilosuchus trinquei*, a new procoelous crocodyliform from the Lower Cretaceous (Albian) Glen Rose Formation of Texas. *Journal of Vertebrate Paleontology*, 23, 128–145.

RÖHL, U., WESTERHOLD, T., BRALOWER, T. J. and ZACHOS, J. C. 2007. On the duration of the Paleocene-Eocene thermal maximum (PETM). *Geochemistry, Geophysics, Geosystems*, 8.

ROOS, J., AGGARWAL, R. K. and JANKE, A. 2007. Extended mitogenomic phylogenetic analyses yield new insight into crocodylian evolution and their survival of the Cretaceous-Tertiary boundary. *Molecular Phylogenetics & Evolution*, 45, 663–673.

RUTA, M., WAGNER, P. J. and COATES, M. I. 2006. Evolutionary patterns in early tetrapods. I. Rapid initial diversification followed by decrease in rates of character change. *Proceedings of the Royal Society B*, 273, 2107–2111.

SALISBURY, S. W., MOLNAR, R. E., FREY, E. and WILLIS, P. M. A. 2006. The origin of modern crocodyliforms: new evidence from the Cretaceous of Australia. *Proceedings of the Royal Society B*, 273, 2439–2448.

SCHWARZ, D. and SALISBURY, S. W. 2005. A new species of *Theriosuchus* (Atoposauridae, Crocodylomorpha) from the Late Jurassic (Kimmeridgian) of Guimarota, Portugal. *Geobios*, 38, 779–802.

SCHWARZ, D., RADDATZ, M. and WINGS, O. 2017. *Knoetschkesuchus langenbergensis* gen. nov. sp. nov., a new atoposaurid crocodyliform from the Upper Jurassic Langenberg Quarry (Lower Saxony, northwestern Germany), and its relationships to *Theriosuchus*. *PLoS One*, 12, e0160617.

SELLWOOD, B. W. and VALDES, P. J. 2008. Jurassic climates. *Proceedings of the Geologists' Association*, 119, 5–17.

SERENO, P. C. 2007. Logical basis for morphological characters in phylogenetics. *Cladistics*, 23, 565–587.

SERENO, P. and LARSSON, H. 2009. Cretaceous crocodyliforms from the Sahara. *ZooKeys*, 28, 1–143.

SERENO, P. C., LARSSON, H. C. E., SIDOR, C. A. and GADO, B. 2001. The giant crocodyliform *Sarcosuchus* from the Cretaceous of Africa. *Science*, 294, 1516–1519.

SMITH, A. B. 1994. *Systematics and the fossil record: Documenting evolutionary patterns*. Blackwell Science.

SMITH, D. K., ALLEN, E. R., SANDERS, R. K. and STADTMAN, K. L. 2010. A new specimen of *Eutretauranosuchus* (Crocodyliformes; Goniopholididae) from Dry Mesa, Colorado. *Journal of Vertebrate Paleontology*, 30, 1466–1477.

SOLÓRZANO, A., NÚÑEZ-FLORES, M., INOSTROZA-MICHAEL, O. and HERNÁNDEZ, C. E. 2019. Biotic and abiotic factors driving the diversification dynamics of Crocodylia. *Palaeontology*, 63, 415–429.

SOOKIAS, R. B. 2020. Exploring the effects of character construction and choice, outgroups and analytical method on phylogenetic inference from discrete characters in extant crocodilians. *Zoological Journal of the Linnean Society*, 189, 670–699.

SOUL, L. C. and FRIEDMAN, M. 2017. Bias in phylogenetic measurements of extinction and a case study of end-Permian tetrapods. *Palaeontology*, 60, 169–185.

SPRINGER, M. S., MEREDITH, R. W., JANECKA, J. E. and MURPHY, W. J. 2011. The historical biogeography of Mammalia. *Philosophical Transactions of the Royal Society B*, 366, 2478–2502.

STADLER, T. 2010. Sampling-through-time in birth–death trees. *Journal of Theoretical Biology*, 267, 396–404.

STOCKDALE, M. T. and BENTON, M. J. 2021. Environmental drivers of body size evolution in crocodile-line archosaurs. *Communications Biology*, 4, 1–11.

STORER, J. E. 1993. Additions to the mammalian paleofauna of Saskatchewan. *Modern Geology*, 18, 475–487.

STROMER, E. 1933. *Ergebnisse d. Forschungsreisen Prof. E. Stromers in d. Wüsten Ägyptens. II. Wirbeltierreste d. Baharije-Stufe (unterstes Cenoman). 12. Die procölen Crocodilia*. Abhandlungen der Bayrischen Akademie der Wissenschaften. Mathematisch-naturwissenschaftliche Abteilung. Bayrischen Akademie der Wissenschaften, Munich.

STUBBS, T. L., PIERCE, S. E., ELSLER, A., ANDERSON, P. S. L., RAYFIELD, E. J. and BENTON, M. J. 2021. Ecological opportunity and the rise and fall of crocodylomorph evolutionary innovation. *Proceedings of the Royal Society B*, 288, 20210069.

SWEETMAN, S., PEDREIRA-SEGADE, U. and VIDOVIC, S. 2014. A new bernissartiid crocodyliform from the Lower Cretaceous Wessex Formation (Wealden Group, Barremian) of the Isle of Wight, southern England. *Acta Palaeontologica Polonica*, 60, 257–268.

TENNANT, J. P., MANNION, P. D. and UPCHURCH, P. 2016a. Sea level regulated tetrapod diversity dynamics through the Jurassic/Cretaceous interval. *Nature Communications*, 7, 12737.

TENNANT, J. P., MANNION, P. D. and UPCHURCH, P. 2016b. Environmental drivers of crocodyliform extinction across the Jurassic/Cretaceous transition. *Proceedings of the Royal Society B*, 283, 20152840.

TOLJAGIĆ, O. and BUTLER, R. J. 2013. Triassic–Jurassic mass extinction as trigger for the Mesozoic radiation of crocodylomorphs. *Biology Letters*, 9, 20130095.

TURNER, A. H. 2015. A review of *Shamosuchus* and *Paralligator* (Crocodyliformes, Neosuchia) from the Cretaceous of Asia. *PLoS One*, **10**, e011811.

TURNER, A. H. and PRITCHARD, A. C. 2015. The monophyly of Susisuchidae (Crocodyliformes) and its phylogenetic placement in Neosuchia. *PeerJ*, **3**, e759.

TURNER, A. H., PRITCHARD, A. C. and MATZKE, N. J. 2017. Empirical and Bayesian approaches to fossil-only divergence times: a study across three reptile clades. *PLoS One*, **12**, e0169885.

TYKOSKI, R. S., ROWE, T. B., KETCHAM, R. A. and COLBERT, M. W. 2002. *Calsoyasuchus valliceps*, a new crocodyliform from the Early Jurassic Kayenta Formation of Arizona. *Journal of Vertebrate Paleontology*, **22**, 593–611.

VENCZEL, M. and CODREA, V. A. 2019. A new Theriosuchus-like crocodyliform from the Maastrichtian of Romania. *Cretaceous Research*, **100**, 24–38.

WILBERG, E. W. 2015. What's in an outgroup? The impact of outgroup choice on the phylogenetic position of Thalattosuchia (Crocodylomorpha) and the origin of Crocodyliformes. *Systematic Biology*, **64**, 621–37.

WILBERG, E. W., TURNER, A. H. and BROCHU, C. A. 2019. Evolutionary structure and timing of major habitat shifts in Crocodylomorpha. *Scientific Reports*, **9**, 514.

WILLIAMSON, T. E. 1996. ?*Brachychampsa sealeyi*, sp. nov., (Crocodylia, Alligatoroidea) from the Upper Cretaceous (Lower Campanian) Menefee Formation, northwestern New Mexico. *Journal of Vertebrate Paleontology*, **16**, 421–431.

WU, X.-C., BRINKMAN, D. B. and RUSSELL, A. P. 1996. A new alligator from the Upper Cretaceous of Canada and the relationship of early eusuchians. *Palaeontology*, **39**, 351–376.

WU, X.-C., RUSSELL, A. P. and BRINKMAN, D. B. 2001*a*. A review of *Leidyosuchus canadensis* Lambe, 1907 (Archosauria: Crocodylia) and an assessment of cranial variation based upon new material. *Canadian Journal of Earth Sciences*, **38**, 1665–1687.

WU, X.-C., RUSSELL, A. P. and CUMBAA, S. L. 2001*b*. *Terminonaris* (Archosauria: Crocodyliformes): new material from Saskatchewan, Canada, and comments on Its phylogenetic relationships. *Journal of Vertebrate Paleontology*, **21**, 492–514.

YOUNG, M. T. and ANDRADE, M. B. DE 2009. What is *Geosaurus*? Redescription of *Geosaurus giganteus* (Thalattosuchia: Metriorhynchidae) from the Upper Jurassic of Bayern, Germany. *Zoological Journal of the Linnean Society*, **157**, 551–585.